April 2014

Designing a Fibrin Scaffold for Lung Resident Mesenchymal Stem Cell Therapy in Emphysema Patients

Alyssa B. Tsiros
Worcester Polytechnic Institute

Kara Ann Negrini
Worcester Polytechnic Institute

Lauren Barbara McCarthy
Worcester Polytechnic Institute

Designing a Fibrin Scaffold for Lung Resident Mesenchymal Stem Cell Therapy in Emphysema Patients

A Major Qualifying Project Submitted to the Faculty of
WORCESTER POLYTECHNIC INSTITUTE
In partial fulfillment for the Degree of Bachelor of Science

Submitted by:

Lauren McCarthy _____

Kara Negrini _____

Alyssa Tsiros _____

Submitted to:

Professor Glenn Gaudette _____

Professor Dave Adams _____

April 29, 2014

Authorship

Each member contributed equally to the completion of this project and editing of the paper. In terms of the writing of this report, some team members held greater responsibility in contributing to specific sections of the paper. Lauren McCarthy was responsible for the Literature Review and Project Strategy, Kara Negrini was responsible for Mechanical Modeling including Methodology and Results sections, and Alyssa Tsiros was responsible for the Gene Expression Methodology and Results. Each team member contributed to reviewing and editing all sections of the paper.

Acknowledgements

We would like to thank Tufts Cummings School of Veterinary Medicine for supplying us with the lab space and resources to complete this project. Specifically we would like to give special thanks to Dr. Andrew Hoffman and Dr. Kristen Thane for their guidance throughout the experimentation; without their help, this project would not have been possible. Furthermore, we would like to acknowledge the staff at Tufts Regenerative Medicine Lab for helping in training and using the equipment within the laboratory. Finally, we would like to thank our WPI advisors Glenn Gaudette and Dave Adams for their support during the duration of this study.

Abstract

Based on promising results seen in regenerative therapies for wound healing, this study explores the use of delivering stem cells through a fibrin hydrogel for the treatment of emphysema, an end stage lung disease. To determine an optimal formulation of the biopolymer fibrin, gene expression of lung resident mesenchymal stem cells (LR-MSCs) was studied in three different scaffold formulations. In addition, mechanical modeling was completed to correlate any uncharacteristic behavior with a change in mechanical properties. The results from the study indicated that a 3 mg/mL concentration of fibrinogen with 500U of thrombin may be optimal over the currently used concentrations in the Hoffman laboratory at Tufts Cummings School of Veterinary medicine; however, additional testing needs to be completed to validate mechanical modeling and demonstrate the potency potential of LR-MSCs on secondary cell lines.

Table of Contents

Table of Figures

Table of Tables

Chapter 1. Introduction

Chronic Obstructive Pulmonary Disease (COPD) is the third leading cause of death in the United States (Epidemiology, 2012). Characterized by the inability to fully exhale, and thus difficulty in breathing and supplying the body with adequate oxygen, emphysema is a type of COPD which is often terminal. Medications such as bronchodilators, steroids, or antibiotics may be prescribed to ease the difficulty of breathing; however, the only long term solution is a lung transplant. The limited availability of transplants, along with donor compatibility, and high rejection rate make lung transplants extremely difficult and costly.

As a result, the area of designing stem cell therapies for COPD has become increasingly popular. A commonly used cell type in regenerative therapies is Mesenchymal Stem Cells (MSCs). MSCs are readily available and can be derived from various parts of the body. Additionally, they are particularly known for their ability to signal adjacent cells through the secretion of unique cytokines as a mode of treatment. Although MSCs derived from bone-marrow (BM-MSCs) have shown potential for regenerative effects, recent isolation of MSCs from adult lung parenchyma has shown better retention in the lung compared to BM-MSCs. Current stem cell therapies for COPD using lung resident MSCs (LR-MSCs) encapsulated in a fibrinogen (3.2%)-fibronectin (0.2%) thrombin hydrogel are being explored through ovine emphysema models at Tufts Cummings School of Veterinary Medicine. However, there are still many questions about the effects of the scaffold on cell signaling for this particular design.

The purpose of this project was to strategically design a biological scaffold for pulmonary regeneration. The potential for such a scaffold will not only increase the likelihood of an effective therapy for COPD patients, but it can also provide insights for which scaffold formulations best induce gene expression profiles in LR-MSCs that correlate with restoration of pulmonary function.

The group chose to pursue a fibrin scaffold and focused on observing changes in gene expression of LR-MSCs within various scaffold groups as well as mechanical modeling to predict whether the fibrin scaffold could withstand or mimic the properties seen in alveolar lung tissue.

Chapter 2. Literature Review

2.1 The Respiratory System

The process of breathing in and out is essential for supplying oxygen to the trillions of cells within the human body. On average, the human respiratory system brings 7L of air/min into the two lungs. Respiration, the process of removing carbon dioxide from the blood and replacing it with oxygen occurs in two stages, gas exchange and cellular respiration. Gas exchange involves the transfer of carbon dioxide and oxygen between the atmosphere and the blood through the pulmonary cavities. The second stage breaks down oxygen by a series of metabolic reactions which release carbon dioxide and energy. This cycle is then repeated, as oxygen is required to provide the initiation of cellular respiration. The respiratory system has many important components that allow it to function properly, such as muscles and an airtight chest wall; however, the lungs are a major component in the system (Rhoades and Bell, 2009).

2.1.1 Lung Structure

The human body contains two lungs, each with numerous lobes. The trachea and first sixteen generations of airway branches are called the conducting zone; this area is responsible for warming and humidifying the air, distributing the air evenly to deeper parts of the lungs and serving as part of the body's defense system against foreign material. The last seven generations include the respiratory zone, which is home to alveolar ducts and 300-500 million alveoli with an internal surface area of $75m^2$ (Rhoades and Bell, 2009). This zone is responsible for the gas exchange and pulmonary circulation. This capillary network has been viewed as the most extensive in the body. The respiratory system is outlined in **Figure 1**.

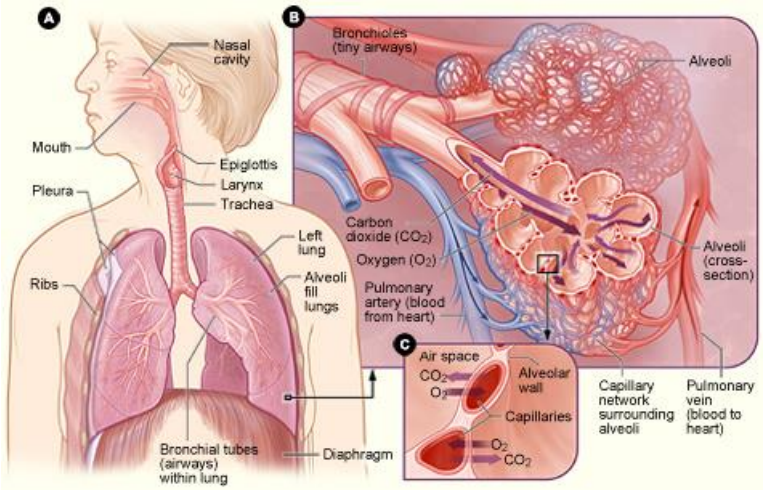

Figure 1. (A) Labelled diagram of respiratory system. (B) Enlarged view of the alveoli and capillaries in the lung. (C) Process of gas exchange between capillaries and alveoli. ("The Respiratory System," 2012)

The mechanics of breathing are controlled by the diaphragm and pressure. Contraction of the diaphragm allows the airtight thoracic cavity to expand and thus inflate the lungs. Although the diaphragm is an essential part in breathing, the process of inflation and deflation of the lungs could not be completed without proper pressure-volume relationships. Because the thoracic cavity is airtight, an increase in volume causes a decrease in pleural pressure, or the pressure in the pleural space between the lungs and chest wall. During normal inspiration, pleural pressure remains negative because the elastic recoil of the lung acts like a spring causing equal and opposite forces between the lung and chest wall. The ability of the lungs to expand and retract is due to the collagen and elastin fibers which form a mesh around the alveolar walls. Elastin fibers can be stretched to nearly double their length, while collagen fibers resist stretch to limit lung expansion. A lung that has lost its elastic recoil becomes easy to inflate but hard to deflate. In order to maintain compliance, the lungs must sustain a constant surface tension throughout changes in pressure and volume. The moist alveolar membrane causes surface tension because water molecules are more strongly attached than air molecules which results in an inwardly directed force that can cause alveoli to collapse. To compensate, the alveolar lining is coated with pulmonary surfactant, a liquid

which lowers surface tension at the interface and changes the surface tension depending on the alveolar diameter. This unique fluid contains dipalmitoylphosphatidylcholine (DPPC), an agent that makes it possible for alveoli of different sizes to survive at low lung volumes (Hoehm and Marieb, 2013; Rhoades and Bell, 2009).

Although there are over 40 types of cells in the lung, two unique cells are alveolar type I and type II cells. Alveolar type II cells, also called type II pneumocytes, are responsible for the synthesis of surfactant. These cells are rich in mitochondria and contain electron-dense lamellar inclusion bodies which are thought to be the storage sites for surfactant. Although the ratio of type I to type II cells is about 1:1, type I cells occupy about two-thirds of the alveolar surface (Rhoades and Bell, 2009).

2.1.2 Lung Biomechanics

Because the lungs are constantly inhaling or exhaling, the tissues are always subjected to tensile stress. This stress, also known as prestress, is a result of transpulmonary pressure. It is distributed throughout the lung by interaction of the extracellular matrix (ECM) and the collagen in the lung. Collagen is the main load-bearing component of all connective tissue; therefore, it is responsible for transferring stresses to the ECM. Mechanical testing has found the Young's modulus of an alveolar wall to be approximately 5 kPa (Suki et al., 2005).

The forces within the lung depend on lung compliance and the current volume of the lung. Since lung volume increases with inhalation, lung compliance also increases, thus increasing the forces within the lungs. Calculations based on the compliance equation, $C = V / P$, where V= volume and P= pressure, revealed a maximum force of 7.68 N and a resting force of 5.11 N over a 9.60 cm^2 area. These values are consistent with Mijailovich et al.'s (1994) study in a rabbit lung. Mijailovich et al. measured a maximum force of approximately 6 N.

In emphysema patients, both forces within the lung and Young's modulus are affected. Due to the inability to fully exhale, there are mechanical changes in the alveolar wall. This consequently causes the lung to respond to changes in deformation differently. Overall, this could lead to deviations in the way the ECM interacts with other molecules (Suki et al., 2005).

2.1.3 Measuring Lung Function

Pulmonary function tests may be used to quantify whether the lung is functioning properly. Spirometry is a procedure used to measure the volume of air inspired or expired by the lungs. These devices can be used to measure the maximum amount of air in the lung (vital capacity), the volume of air remaining in the lungs after expiration (functional residual capacity), and the volume of air when expiration is performed rapidly (force vital capacity) (Townsend, 2011). **Figure 2** shows how results of spirometry are quantified so that they can be compared for patients based on expected values given height, age and gender. Generally, a healthy result is >80% of the predicted value, while abnormal results are 60-79% for mild lung dysfunction, 40-59% for moderate lung dysfunction, and <40% for severe lung dysfunction (Boriello et al., 2012).

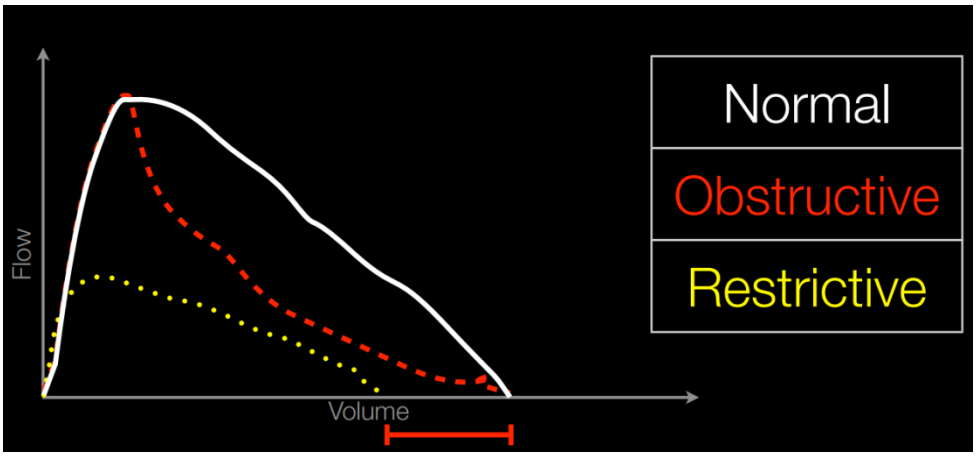

Figure 2. Flow vs. Volume graphs can be used to determine several values such as FVC, FEV1, FEV1/FVC and PEF. Based on the curve result, spirometry can be used to classify types of lung diseases (Boriello et al., 2012).

2.1.4 Respiratory Disease

According to the Center for Disease Control and Prevention, 10.1 million (4.4%) adults in the U.S. have been diagnosed with chronic bronchitis within the past year, and 4.7 million (2.0%) have been diagnosed with emphysema (CDC, 2013), the prevalence data are shown in **Figure 3**. Chronic obstructive pulmonary disease (COPD) constitutes a group of lung diseases all caused by the obstruction of airways which impacts breathing ability; in fact, COPD is the third leading cause of death in the U.S. and is predicted to cost about $42.6 billion, including $26.7 billion in direct health care expenditures, $8.0 billion in indirect morbidity costs, and $7.9 billion in indirect mortality costs (Epidemiology, 2012).

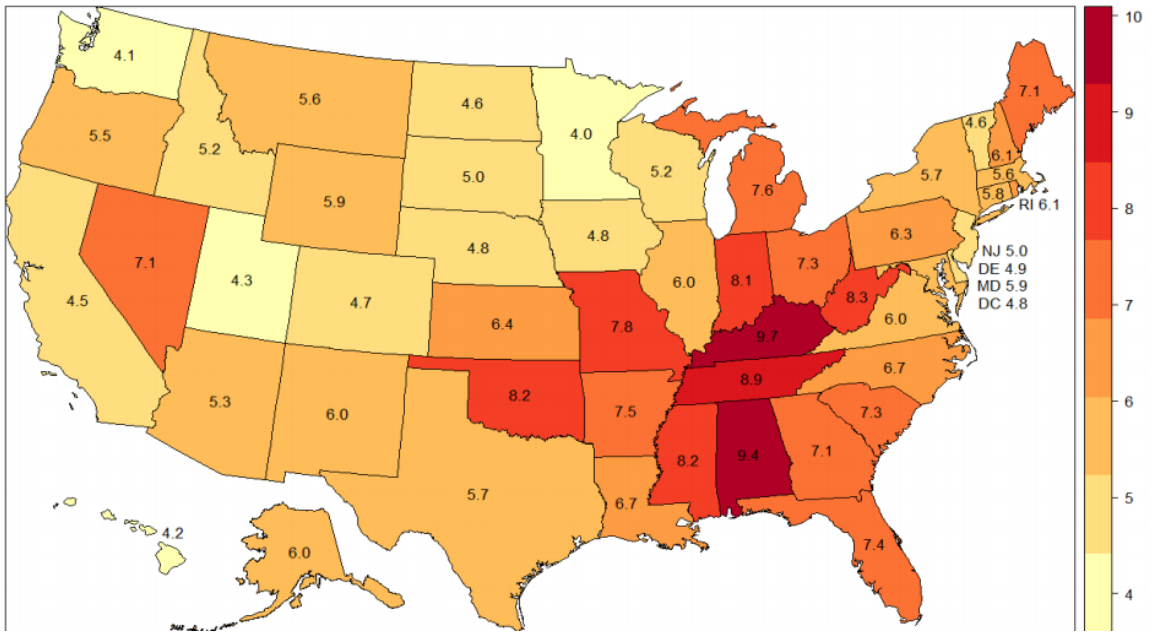

Figure 3. Age adjusted prevalence (%) of adults who answered yes to "Have you ever been told you have COPD, emphysema or chronic bronchitis?" Sources for data taken in 2011 from Centers for Disease Control and Prevention, National Center for Health Statistics, and behavioral Risk Factor Surveillance System (CDC, 2013).

Obstruction of the lungs is characterized in three ways, excess mucus, airway narrowing, or airway collapse during expiration. Subdivisions of COPD include bronchitis, asthma, and emphysema which are all characterized by the slowing down of movement during expiration or the inability for those affected to empty their lungs. Inflammation in one or more bronchi causes

bronchitis and excessive mucus production. The over-distension and loss of elastic recoil in the lungs causes emphysema while spasmodic contractions of the smooth muscle on the bronchi cause asthma. Altogether, these conditions result in a decrease in forced vital capacity and forced expiratory volume. Bronchitis and emphysema often affect the same patient as the mucus caused by bronchitis leads to a severe cough which stretches the lungs and decreases their ability to recoil. The effect of emphysema at the microscale can be seen in histological samples of normal and diseased lung tissue (**Figure 4**). As shown in the images, the normal lung tissue shows a dense alveolar network while the emphysema model shows larger alveoli diameters with reduced alveoli cells which supports the problem seen in emphysema in that the lungs are difficult to empty because of these large air pockets (Schleede et al., 2012). If the disease progresses patients typically experience hypoxemia and hypercapnia which eventually cause right-heart failure.

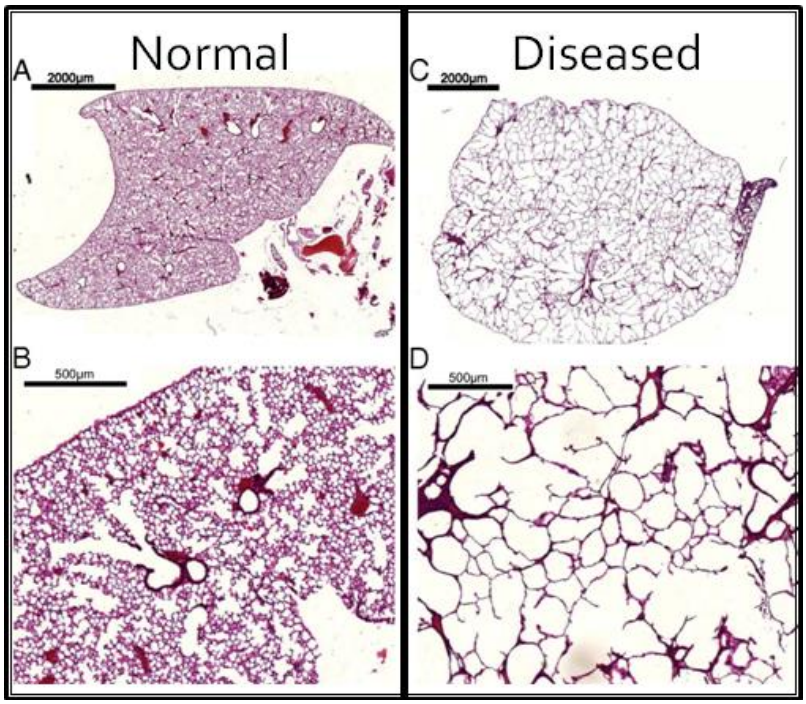

Figure 4. Histological sections in experimental emphysema model give a representation of the typical problems seen in diseased lung tissue at the microscopic level (Schleede et al., 2012).

2.1.5 Treatment Options

Currently, this end-stage lung disease has a limited number of treatment options. In certain cases, doctors may prescribe drugs to ease symptoms. Bronchodilators which work by opening the airways to permit more efficient oxygen exchange in patients with excess mucus can be divided into three different categories: "sympathomimetics (isoproterenol, metaproterenol, terbutaline, albuterol), which can be inhaled, taken by mouth, or injected; parasympathomimetics (atropine); and methylxanthines (theophylline), which may be administered intravenously, orally, or rectally" (Swartout-Corbeil et al., 2011). Other drugs for treating emphysema include steroids (beclomethasone, dexamethasone, triamcinolone, flunisolide) which lower tissue inflammation, antibiotics which may help fight lung infections, and expectorants which loosen mucus in the lungs. An alternative therapy which can increase survival rate in emphysema patients is oxygen therapy which can be administered by portable oxygen tanks but it must be used 18-24 hours every day (Swartout-Corbeil et al., 2011). Surgery may be beneficial for removing parts of the diseased lung to allow for lung volume reduction. Another recently proposed method for lung volume reduction is the use of a polymer sealant to close off damaged areas of the lungs; however, this treatment is still under investigation in clinical trials (Ingenito, 2010). Unfortunately, the closest long term solution to "curing" the disease is a lung transplant, which is not only limited in availability but also poses the risk of rejection, along with a mere 50% five year survival rate and lifelong immune-suppression. Because of the overwhelming need for a new treatment option, scientists have been exploring new therapies using the idea of tissue regeneration to repair damaged lungs.

2.2 Therapies for Lung Regeneration

The regeneration approach originates from the idea that an entire limb, organ, or tissue in the body can be entirely re-grown. The biological process to undergo such a task is quite

complicated as it involves tissue remodeling, reprogramming genes, differentiation, proliferation, and migration of stem cells to the site of interest. Despite the complicated process, stem cell therapy has real potential for future treatment options, not only of the lung but of any body part.

2.2.1 Mesenchymal stem cells

Although there are many types of stem cells, the most widely used is the mesenchymal stem cell (MSC). These multipotent stem cells are readily available, have multi-lineage differentiation potential, secrete large amounts of cytokines and have been shown to have immunosuppressive properties (Weiss, 2010). Originally termed Colony-Forming Unit-Fibroblasts (CFU-F) after demonstrating self-renewal capabilities in bone marrow cells during the 1960s, these cells were later labeled "mesenchymal stem cells" in 1991 (Collins and Thebaud, 2013). Numerous *in vitro* and *in vivo* studies have demonstrated benefits from MSC transplantations; however, despite the promising outlook, few MSCs attach to the target area *in vivo* or they cleared by the body's immune response before the cell can help heal the damaged region (Davis et al., 2011).

2.2.1.1 Characterization

All MSCs must follow a minimum set of criteria. First, when cultured in a flask under standard culturing conditions, MSCs must adhere to the tissue culture plastic. The cells must express the surface markers CD105, CD90, and CD73 and should lack expression of the hematopoietic markers CD45, CD14 or CD11b, CD34, CD19 or CD79a or HLA-DR. Finally, all MSCs must be capable of tri-lineage differentiation into osteogenic, adipogenic, and chondrogenic lineages upon *in vitro* stimulation (Collins and Thebaud, 2013).

2.2.1.2 Types

MSCs can be isolated from stromal tissue of many organs, including bone marrow, muscle, periosteum, adipose, dermis, and lung. These cells have been reported to show high similarity to

other cell types such as perivascular cells and fibroblasts. Perivascular cells (pericytes, PCs) are multi-lineage progenitor cells which differentiate in culture to adherent cells with a specific MSC phenotype. These similarities suggest that PCs may be the progenitors of MSCs. Because of MSCs similarity to other stem cell types, the differences between MSCs derived from various areas of the body has become an interest to scientists in regenerative medicine (Collins and Thebaud, 2013).

2.2.1.2.1 Bone marrow derived mesenchymal stem cells

Bone marrow derived mesenchymal stem cells (BM-MSC) were the first type of MSC to be discovered. The potential of these cells to differentiate into adipocytes, osteoblasts, chondrocytes and other tissues of mesodermal origin has made them extensively analyzed for their possible *in vivo* use (Ricciardi et al., 2012). The cells have been shown to migrate to and remodel lung tissue in healing allografts of lung transplant patients; however, when implanted into animal models of lung disease, the therapy shows little success (Ingenito et al., 2012).

2.2.1.2.2 Lung resident mesenchymal stem cells

Recently, a new line of MSCs has been isolated from adult lung parenchyma. Lung resident mesenchymal stem cells (LR-MSCs) have been shown to produce lung-specific basement membrane proteins such as collagen IV, laminin, and fibrillin-1 and enhance the growth and spreading of epithelial progenitor cells. Furthermore, these cells express greater levels of the intracellular adhesion molecule, PDGFRa, and integrin a2, thus causing increased adherence of LR-MSCs to endothelial cells (Davis et al., 2011). *In vitro*, these cells have been observed to differentiate into epithelial, endothelial and nerve cells. Furthermore, *in vivo* studies in a murine emphysema model found that LR-MSCs demonstrate greater survival and avoidance of blocking antibodies than BM-MSCs after intravenous transplantation. In humans, LR-MSCs exhibited

potential to inhibit T-cell proliferation, thus modulating immune responses (Ingenito et al., 2012; Collins and Thebaud, 2013).

2.2.1.3 Cell Signaling

The ability for cells to function under abnormal conditions stems from their ability to maintain homeostasis. Self-regulation of the body's internal environment is greatly affected by cells ability to communicate with one another in order to respond accordingly to the presented variation. Cells have numerous modes of direct and indirect communication. Stem cells in particular are known for their ability to communicate using indirect signaling. Most notably, they can communicate using paracrine signaling, or by the release of a chemical messenger. Paracrine signaling works by the diffusion of a chemical signal across extracellular fluid to a nearby cell where it binds with high specificity to cell receptors on the plasma membrane of the receiving cell.

MSCs have been shown to serve as an effective therapy for treating lung injury because of their capabilities to signal adjacent cells. Several studies have demonstrated MSCs ability to modulate the immune system by releasing immunosuppressive factors such as prostagladin E-2 (PGE-2) in response to dendritic cells, T and B cells, and neutrophils. More importantly, LR-MSCs have shown the ability to secrete growth factors such as vascular endothelial growth factor (VEGF), keratinocyte growth factor (KGF), and hepatocyte growth factor (HGF) which have cytoprotective and repair properties (Fitzgerald et al., 2001). Although it is unknown which cytokines impact injured cells the most, the importance of creating a therapy that allows for or encourages cell signaling is evident for MSCs.

This project will investigate the effects of various cell scaffolds on the gene expression profiles of LR-MSCs. Seven gene expression candidates were carefully chosen for analysis, and are described below (two are of the FGF type).

2.2.1.3.1 Vascular Endothelial Growth Factor

Vascular Endothelial Growth factor (VEGF) plays a role in vascular development, specifically during embryogenesis (vasculogenesis) as well as blood-vessel formation (angiogenesis). This heparin-binding, dimeric protein also acts as a mitogen for endothelial cells, and plays a role in activating and chemo-attracting monocytes. VEGF belongs to a family of proteins including VEGF-A, VEGF-B, VEGF-C, VEGF-D and placenta-like growth factor (PLGF).The ability for VEGF to stimulate endothelial cells to proliferate, migrate, and survive in an altered environment has caused increasing interest into how and why cells excrete this factor. VEGF-A, a 23 kDa glycoprotein and one of the more common forms of VEGF in humans has five different isoforms (Breen, 2007). VEGF-B has been associated with regulation of extracellular matrix degradation, cell adhesion and migration. VEGF mRNA expression studies in the heart, placenta, ovary, small intestine, and the thyroid gland suggest that VEGF-C may play a role in proliferation of blood and lymphatic vascular endothelial cells. Platelet-derived growth factor-B, epidermal growth factor, tumor necrosis factor alpha (TNF-α), transforming growth factor-beta 1 (TGF-β1) and interleukin-1β have been shown to induce the transcription of VEGF mRNA (Veikkola and Alitalo, 1999).

2.2.1.3.2 Fibroblast Growth Factor

First discovered as a family of proteins capable of promoting fibroblast proliferation, fibroblast growth factors (FGFs) have been shown to modulate cell proliferation, motility, differentiation, and angiogenesis. These molecules are a family of ligands which include twenty-two members in humans and mice. Often found on the extracellular matrix, these ligands have a high affinity for heparin. Depending on the cell-type, FGF signaling can have different effects (Dailey et al., 2005). FGF signaling has also been shown to be important in embryonic

development in both mouse and human genetics as it orchestrates development by instructing uncommitted cells to proliferate and differentiate into specific lineages.

2.2.1.3.3 Hepatocyte Growth Factor

Hepatocyte growth factor (HGF) is primarily known for being a growth factor that functions in liver regeneration. However, recent evidence shows that HGF is a multipotent growth factor involved with regeneration and maintenance of multiple types of tissues and organs. More specifically, HGF assists in mitosis for epithelial cells, endothelial cells, stromal cells, and some carcinoma cells. It is also involved with hematopoiesis by stimulating the proliferation of progenitor cells. HGF can increase cell motility and angiogenesis. Because of this characteristic, there is belief that HGF plays a role in tumor cell growth, invasion and metastasis. There is also evidence that HGF is involved in chondrogenesis and bone remodeling (Matsumoto and Nakamura, 1996).

One study in particular observed HGF regulation and signaling in hematogenous spreading of cancer cells. They found that there was increased HGF expression at both the RNA and protein levels, suggesting an important role in promoting epithelial-mesenchymal transition, or cell migration (Ogunwobi et al., 2013). In contrast, in human mesenchymal stem cells (hMSCs), HGF is down-regulated by the production of transforming growth factor-β. Because of this interaction and the production of HGF by activated macrophages, one study notes that HGF production can be regulated by the microenvironment. Overall, HGF levels are higher at injured tissue sites (Neuss et al., 2004).

2.2.1.3.4 Transforming Growth Factor

Transforming growth factor-beta1 (TGF-β1) is a part of a family of cytokines involved with growth and development. Recent studies have shown that macrophages, and B and T lymphocytes secrete TGF-β1 (Assoian et al., 1987; Kehrl et al., 1986; Kehrl and Wakefield et al.,

1986; Chantry et al., 1989). From this, it can be predicted that TGF-β1 also has a role in immunoregulation. More specifically, TGF-β1 has a role in the immune system through inhibiting various factors such as interleukin expression; B lymphocyte, T lymphocyte, and thymocyte proliferation; antibody production; natural killer cell generation, and cytotoxic T cell generation (Kehrl and Wakefield et al., 1986; Shalaby and Ammann, 1988; Ellingsworth et al., 1988; Rook et al., 1986; Ranges et al., 1987; Chantry et al., 1989) This immunoregulatory function helps explain why TGF-β1 can play a significant role in chronic allograft dysfunction. Studies where TGF-β1 genes are overexpressed have shown that there is an increased risk of organ rejection after transplantation (Pribylova-Hribova et al., 2006).

2.2.1.3.5 Angiopoietin-1

Angiopoietin-1 (ANG1) is a proangiogenic growth factor which has been seen to induce distinctive vascular remodeling. Although angiogenic growth factors such as basic fibroblast growth factor, vascular endothelial growth factor, and hepatocyte growth factor have been explored for ischemia, their ability to promote neovascularization has been outweighed by the unwanted side effects of accelerated inflammation and fibrosis. As a result, ANG1 has been explored for therapeutic neovascularization. It has been found that systemic or topical application of ANG1 accelerates wound closure and epidermal/dermal regeneration through enhanced angiogenesis, and increased blood flow in the wound region of *db*/*db* diabetic mice (Koh, 2013).

2.2.1.3.6 Insulin-like Growth Factor

Insulin-like growth factor (IGF) is a growth factor secreted by many different tissues in the body, and thus has different forms. There have been many studies done that connect IGF-I to somatic growth and IGF-II to fetal growth (Stewart and Rotwein, 1996). However, it has been shown that the functions IGF are determined by the cell secreting it. For instance, IGF-I when

secreted from the liver behaves similarly to an endocrine hormone. On the other hand, when being secreted by cells such as cartilage cells, it acts as a paracrine hormone. Additionally, there have been studies connecting IGF to cancer. When involved with cancer it has been found that the growth factor acts in an autocrine manner (Laron, 2001).

2.2.2 Scaffolds

Biocompatible scaffolds offer a newfound way to enhance the capabilities of stem cells. Whether for drug or cell delivery, these scaffolds act as carriers for the treatments. Derived from natural sources, natural polymers offer biocompatibility, controlled degradation, and protection for the therapy being delivered. Fibrin, alginate, collagen, and chitin are the four commonly used natural polymers.

Although biomaterials can be derived from various different materials, biocompatibility, biodegradability, mechanical properties, surface properties, and manufacturing are all important considerations when determining the right biomaterial. For applications of stem cell therapy, tissue engineering often requires designing an artificial extracellular matrix to protect and encourage attachment and proliferation of cells for *in vivo* therapies. The recipe for a successful scaffold requires proper proportions of balancing mechanical strength with biocompatibility. For applications of soft tissues, hydrogels offer high water content, biocompatibility and similar mechanical properties.

One growing area of interest has been in working to characterize scaffold materials in terms of mechanical properties and then observe how cells behave and interact on or within the different surfaces. One type of testing which is commonly used for hydrogels is rheometry. Rheometry measures the deformation and stress on a material by subjecting it to shear stresses.

2.2.2.1 Fibrin

One biopolymer, fibrin, has been used for numerous stem cell therapies. An important component in blood clotting, fibrin monomers form a network of fibers designed for trapping red blood cells, leukocytes, and platelets to stop bleeding by forming a stable clot. The polymerization process can be seen in **Figure 5**. By changing certain factors or component concentrations, the polymerization dynamics can be modified (Puente and Ludena, 2014).

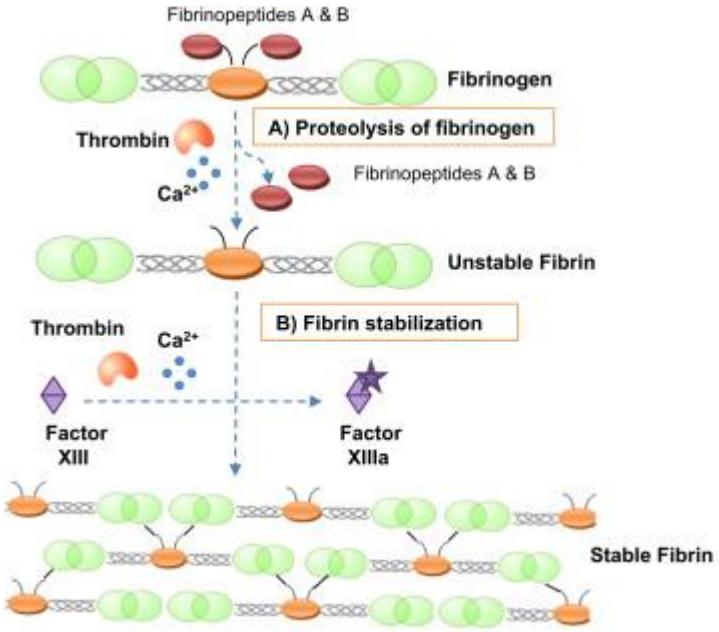

Figure 5. Formation of a fibrin clot by polymerization (Puente and Ludena, 2014).

For example, changing the catalyst (thrombin) concentration can affect the speed of polymerization and branching whereas changing factor XIIIa will affect the degree of crosslinking (Brown & Barker, 2014). The use of this polymer has recently been seen in numerous stem cell strategies to provide protected targeted delivery. For example, a fibrinogen (3.2%)-fibronectin (0.2%)-thrombin hydrogel has previously been studied using autologous lung multipotent stromal cells and has helped facilitate 90% LR-MSC survival after four days. However, the strength of this engraftment is unknown (Ingenito et al., 2012).

Fibrin is a viscoelastic material with unique mechanical properties. Characterizing elastic materials is usually done using Hooke's law which states that the strain or deformation is proportional to the stress of force applied per area; however, the stress is independent from the rate of strain. Viscous materials are characterized by Newton's law which states that stress is proportional to the rate of strain but independent from the strain itself. Unfortunately, viscoelastic materials such as fibrin are characterized by two different parameters, one for elastic properties and the other for the viscous properties. These properties are typically measured by applying a known stress and determining the resulting stain based on the distortion of the polymer. Values seen before in fibrin gels were 50.85-133 kPa (Ahlfors & Billiar, 2007; Linnes et al., 2007) for ultimate tensile strength and 28.56-26.69 KPa for Young's modulus (Huang et al., 2010).

Chapter 3. Project Strategy

After completing a comprehensive literature review, it was well established that there is a gap in knowledge regarding how scaffolds affect cell signaling and biomechanics, even though cell signaling is important to cell survival, engraftment, and potency. Although previous studies at Tufts Cummings School of Veterinary Medicine have used a 3.2%-fibronectin(0.2%)-thrombin hydrogel which showed 90% MSC survival after 4 days, little work has been completed regarding how the scaffold environment affects stem cell potency in terms of gene expression. Furthermore, the mechanical properties of this fibrin scaffold have not been quantified to determine whether the scaffold matches the mechanical properties of the lungs or is even able to withstand the pressures seen in the lungs.

3.1 Initial Client Statement

The original client statement was to invent something that could impact the entire field of regenerative medicine. The goal was to, develop a scaffold that could:

(1) Preserve or enhance the potency of signals released by stem cells (including paracrine signals and exosomes/'microvesicles')

(2) Optimize delivery of those signals to adjacent (in contact or not in contact) cells at microscalar level

(3) Have potential for repository function after transplantation (i.e. sponge-like)

(4) Maintain survival of encapsulated cells for short period after transplantation (i.e. protects cell from immediate death or phagocytosis from innate immune system)

(5) Is safe for delivery into animals/people

3.2 Revised Client Statement

Given the immense undertaking that such a scaffold design would require, along with the unknowns as to what determines an ideal scaffold, the client statement was revised to focus on

evaluating the effect of scaffold material on stem cell potency in terms of gene expression while also ensuring that the mechanical properties of the scaffold mimicked that of healthy lung tissue.

3.3 Objectives

In order to develop an effective scaffold for pulmonary regeneration, a few objectives needed to be met. As determined by the team, the scaffold needed to:

- Be composed of biocompatible & biodegradable material
- Allow for localized cell delivery
- Be easy to handle and formulate
- Maintain or increase gene expression
- Have similar dynamic compliance to healthy lung tissue
- Be safe for use in animals and humans

3.3.1 Ranked Objectives

The image below shows a pairwise comparison chart for ranking the previously stated objectives. This was completed by the team and Dr. Andrew Hoffman of Tufts Cummings Veterinary School of Medicine Regenerative Medicine Laboratory (**Figure 6**).

Objective	Biocompatible	Localized delivery	Easy to handle	Maintain gene expression	Similar dynamic compliance	Total Score
Biocompatible	x	1	1	1	1	4
Localized delivery	0	X	1	1	1	3
Easy to handle	0	0	x	1/2	0	1.5
Maintain gene Expression	0	0	1/2	x	1	1.5
Similar dynamic compliance	0	0	1	0	x	1

Figure 6. Pairwise comparison chart for scaffold objectives.

3.4 Functions

The scaffold also needed to complete numerous tasks. It had to support cell viability and growth factor secretion, mimic biomechanic properties of the lung, and maintain or increase gene expression levels similar to control MSCs of pre-determined growth factors.

3.5 Specifications

To be deemed successful, specifications were determined. Experimental groups needed to have valid control groups to compare the data. Additionally, a method for preventing cell adhesion to the petri dish needed to be completed to prevent invalid data caused by cell adhesion to the proteins attached to the petri dish from the media. To encompass the effect of gene expression over time, sampling points were specified as 0, 1, 4, 24 and 48 hours. To further investigate the changes in gene expression of LR-MSCs, particular genes of interest were chosen based on literature findings supporting the importance of these genes. The following seven genes were chosen for analysis: VEGFA, ANG1, TGF-B, HGF, FGF7, FGF2 and IGF. Finally, through mechanical modeling, the scaffold should show a Young's modulus of 5 kPa +/- 0.1 kPa which was determined by the Young's modulus of a single alveolar wall (Suki et al., 2005).

3.6 Constraints

The scaffold needed to be developed within a few constraints. First, resources were limited to those available and widely used in the Regenerative Medicine Lab at Tufts Cummings School of Veterinary Medicine. Specifically, testing was restricted to the available human stem cell lines. Since the scaffold is to be used *in vivo*, it needed to withstand testing at body temperature (37°C). Furthermore, to get quality mRNA, a minimum concentration of $0.5x10^6$ cells/mL was required.

3.7 Project Approach

In order to fulfill the goals set forth above, the team considered technical, management, and financial aspects.

3.7.1 Technical

To design a biological scaffold which met the criteria outlined above, considerations needed to be made regarding designing test methods to effectively characterize the scaffold in terms of mechanical parameters and subsequent effects on gene expression. Two separate

approaches were used, firstly, gene expression was completed using qPCR and mechanical modeling was done based on viscoelastic linear modeling and data seen in previous studies. The gene expression studies were done *in vitro* using LR-MSCS and the scaffold material. To avoid adherence as previously addressed as a specification, the control groups were cells suspended in media in conical tubes and cells in agar. The studied groups were divided into the experimental groups of LR-MSCs within different scaffold concentrations and control groups of LR-MSCs alone and LR-MSCs in agar to mimic a 3D environment.

For *in vitro* testing, the scaffold concentration ratio was changed by keeping the fibrinogen constant (3 mg/mL) and varying the thrombin concentration. The three experimental groups were 0.5x, 1x, and 2x which were 500U, 1000U and 2000U thrombin with 3 mg/mL fibrinogen respectively. Time points were chosen as t=0 for cells immediately removed from tissue culture plastic as a baseline comparison point, t=1, t=4, t=24 and t=48 hours for the experimental and control groups. At these points, gene expression was analyzed using qPCR to analyze seven carefully chosen targets: VEGFA, HGF, TGF-B1, ANG1, FGF2, FGF7 and IGF.

3.7.2 Management

Time management is key to meeting objectives in an acceptable time frame. The gantt chart shown in **Figure 7** demonstrates the team's plan for the project.

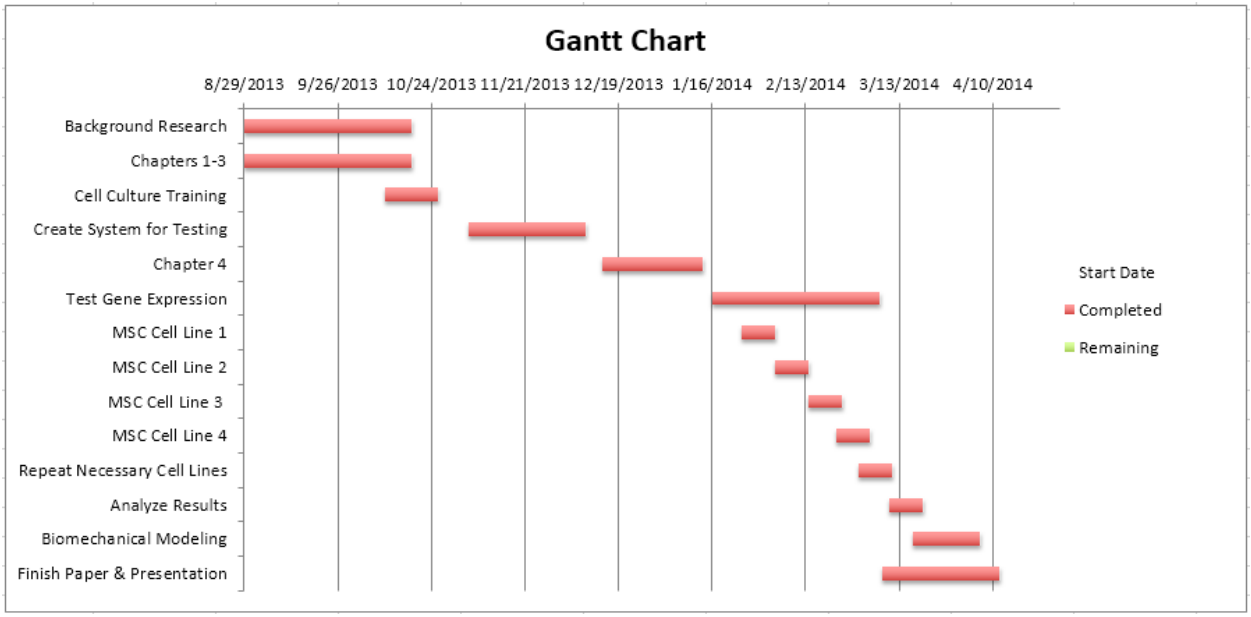

Figure 7. Basic project timeline for August 2013 to May 2013.

3.7.3 Financial

Both materials and methods needed to be evaluated for cost. With a total budget of $468, financial considerations needed to be made regarding the cost of materials and methods. **Table 1** below gives an approximate cost analysis for materials and methods.

Table 1. Approximate materials and methods for experiments using the model system. Costs are shown per unit because the final cost is dependent upon to number of test required (estimates taken from Sigma Aldrich, Life Technologies, and BioTechniques).

Material	Unit	Cost per Unit
Human lung-resident MSCs	n/a	n/a
Scaffold	n/a	n/a
Fibrinogen	100 mg	50
Thrombin	1mL	204
Low adherence plates	24 pc	300-350
Ex-vivo lung	n/a	n/a
Method		
PCR	n/a	450
Loading dye	n/a	50
dNTPs	1000 ul	50
enzyme & buffers	n/a	50

Primers	1 primer	10
ethidium bromide	1 gram	40
TBE buffer	4 liters	50
Agar	500 g	200
ELISA	1 kit	500-600
Western Blots	1 kit	100-200
Immunochemistry	antibody	250-350
Total	-	$2304-2654

Exact costs depend on the number of materials and tests needed. Thankfully, most of the project costs will be covered by an ongoing grant at Tufts Cummings School of Veterinary Medicine.

Chapter 4. Design

As previously discussed, fibrin was chosen as the delivery scaffold for human derived LR-MSCs. Based on the specificity of the design parameters, the concentration of thrombin was changed and three experimental groups were used. The groups all contained 3mg/mL fibrinogen mixed with either 500 U, 1000 U or 2000 U of thrombin. Prior to the team's decision to pursue fibrin as the ideal biological scaffold, design alternatives were considered.

4.1 Design Alternatives

When generating ideas to address the final client statement, numerous alternative designs were proposed. The scaffold material was a huge consideration in designing a new scaffold. Only natural biomaterials were considered; such as collagen which is a major extracellular matrix component in the lung. However, fibrin was chosen based on its involvement in the coagulation cascade during wound healing and based on previous studies supporting the use of fibrin as a delivery vehicle for vascularized areas. Altering the material properties by changing the degree of crosslinking or branching within polymer scaffolds was also considered as a method to potentially create a scaffold which would meet the mechanical properties seen in the lung. Increasing the cell density was also proposed to improve the potency of the therapy; however, this was not seen as being feasible due to the resulting increase in cost. Likewise, the addition of growth factors such as VEGF or HGF could improve the wound healing response in the lung but would be too expensive to implicate and choosing one growth factor would be difficult given the thousands of cytokines and their diverse functions.

Chapter 5. Methodology

To evaluate the therapeutic potential of a fibrin scaffold for delivering LR-MSCs, gene expression testing and mechanical modeling was completed. The cells in the scaffold (3mg/mL fibrinogen and 1000 U thrombin) compared to the cells in agar at 24 hours can be seen in **Figure 8** below. As shown, the cells in the scaffold appear much healthier than the cells in agar because they are branching and forming microtubules to form cell-cell interactions. Although the images show no viability staining, both of these cells were alive at 24 hours because gene expression was completed.

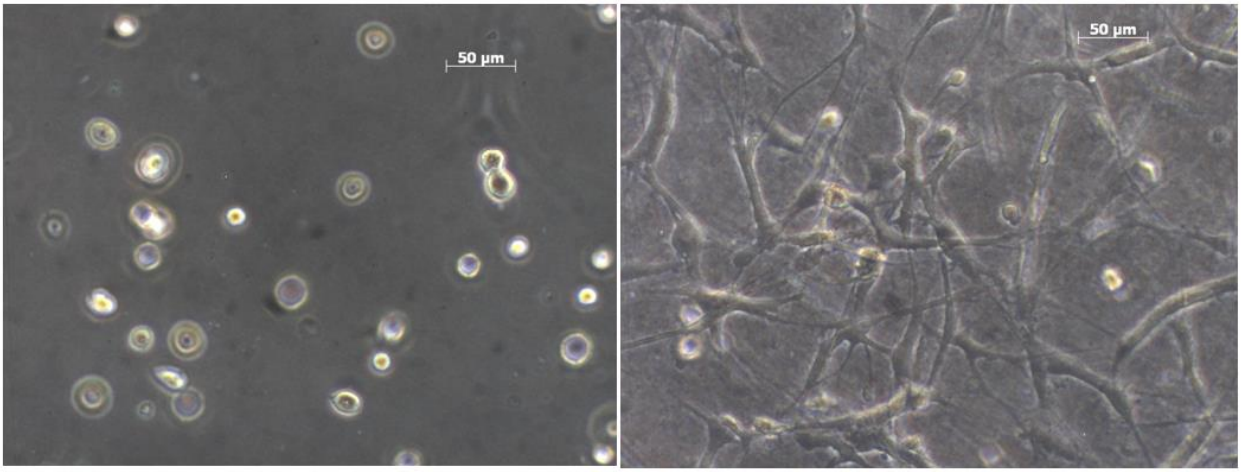

Figure 8. Cells in agar on the left versus cell in the scaffold group with 3mg/mL fibrinogen and 1000 U thrombin on the right.

5.1 Gene Expression

Four LR-MSC lines were chosen for gene expression analyses: H1, H2, H4 and H8 (H8 was run twice, the first run was H8 and the second was H8b). All lines concurrently exhibited appropriate tri-lineage differentiation (osteocytes, chondrocytes and adipocyctes when grown in differentiation media). Cells at passage 2 were stored in liquid nitrogen, thawed at 37°C and then plated on 150mm plates at a density of 500,000 to one million cells per plate. Alpha-MEM containing 10-15% Hyclones FBS and 1x Penicillin/Streptomycin/L-glutamine (P/S/L) was used as medium, and the plates were maintained in a 37°C incubator with 5% CO_2. The medium was

changed every 2-3 days until the cells were grown to near-confluence (70-90% confluence) over 4-6 days. At 12-18 hours prior to scaffold experiments, the FBS-containing medium was removed and the plates were washed twice with PBS and serum free medium was applied with 1x P/S/L. On the day of the scaffold experiments, the cells were lifted from the plates (passage 3 for the scaffold experiments) using Tryp-LE (5mL/plate, incubated at 37°C for 4 minutes, neutralized with 10mL serum-free media/PBS). Cell counts were performed manually using Trypan blue staining and a hemocytometer (20µl cell suspension and 20µl Trypan blue and 80µl medium. Cell counts were completed using the formula: Total cells/mL = (#cells in a 4x4 grid)*(6)*(10^4). One cell line was prepared in the above fashion per week.

5.1.1 Experimental Set-up

Scaffold experiments were performed in 6-well plates with one plate per time point and 3 or 4 plates per cell line (t= 1 hour, 4 hours, 24 hours and 48 hours). The sample placements are shown in **Figure 9**. Control cells were maintained in 15mL conical polypropylene tubes. Fibrinogen was diluted 1:20 with PBS (1 mL full concentration BAC2 mixed with 19mL PBS to get a total volume of 20mL). The experimental and control groups were prepared so that they contained:

S0.5x: 62.5 U and 1 mL fibrinogen/cell suspension
S1x: 125 U and 1mL fibrinogen/cell suspension
S2x:250 U thrombin and 1 mL fibrinogen/cell suspension
Agarose: 1 mL 2% agarose/cell suspension
Cells alone: 1 mL serum-free media/cell suspension

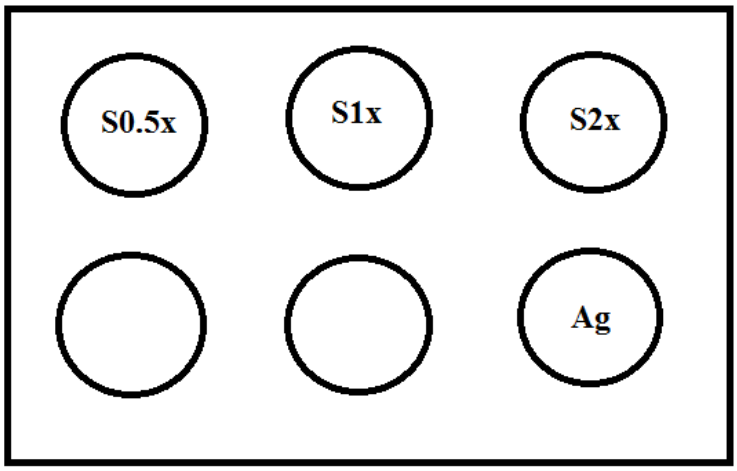

Figure 9. Representative image of the 6-well plate set-up.

5.1.2 Scaffold Experimentation

The following sequence of events was followed for scaffold experimentation. Thrombin was pipetted into three wells per plate as shown in **Figure 9** above and was evenly distributed over the surface of the well using a sterile spreader. The wells were allowed to dry in the hood. Cells were lifted from their plates and counted. Aliquots were separated for resuspension in agarose, fibrinogen or conical tubes depending on the group. Cells were then resuspended at one million cells/mL in 37°C 2% agarose and aliquots of 1mL were placed in one well of six well plate. Plates were wrapped in parafilm and placed within a clean refrigerator (4°C) for 10 minutes to allow the agarose to set. Another aliquot of cells were resuspended at a concentration of one million cells/mL in warm (temperature not measured; between room temperature and 37°C) dilute fibrinogen. The six-well plates were removed from the refrigerator and one mL of fibrinogen/cell suspension was added to each thrombin-coated well. The plates were maintained at 37°C for 15-30 minutes to allow the scaffolds to polymerize prior to lifting the scaffolds from the bottom of the plates (to minimize cells adhering to the plastic of the plate). The cells in agarose could not be lifted because they were too delicate. Five mL of serum-free media was added to each well

containing the scaffold and agarose. Aliquots of one million cells were separated into 15 mL polypropylene tubes and brought to a total volume of one mL with serum-free media.

For cell lines H2 and H8b, an additional test was run using aliquots of cells to observe whether the cells in media alone would behave differently if they were spread over a large surface area. For H2 cells, plates were prepared by coating each well with dextran to minimize binding (one million cells were placed in each of the wells in one mL of media and treated the same as the cell suspensions). For H8b cells, one million cells were placed within the flat polypropylene caps of the 50mL conical tubes and these caps were then placed in a large petri dish.

5.1.3 RNA Sample Preparation

At each time point, the same procedure was followed for each group within each cell line. For the experimental groups, the scaffolds were gently removed from their wells and placed into labeled 50 mL conical polypropylene tubes with efforts to minimize the amount of media taken with the sample. However, for 48 hour scaffolds, most of the mechanical integrity had been broken down so the entire scaffold could not be simply lifted from the tubes. As a result, the full contents of the wells were collected in 15 mL conical tubes and centrifuged (1500 rpm for five minutes). The supernatant was then removed and the cell pellet was resuspended in Trizol for RNA extraction. For the agarose well, media was gently aspirated from the well using manual pipetting and the gel was then moved into a 50 mL conical polypropylene tube for processing. Trizol (Life Technologies, Cat. No. 15596), was added to each sample in the following volumes: 2.5mL Trizol to all intact scaffold groups, 2.5mL Trizol to non-intact scaffold "pellet" groups, 2.0mL Trizol to the 1 mL cell suspension, 2.5mL Trizol to the agarose groups and 0.5mL Trizol to the t=0 baseline samples which were only 100-200µL total volume of cells suspensions. All samples were incubated with Trizol for approximately 30 minutes. Following incubation, homogenization (using a disposable homogenizer) was performed on all scaffold and agarose samples. Control cell

suspensions were briskly pipetted and agitated but not homogenized. The samples were either immediately processed for RNA extraction of frozen at -80°C until processing.

5.1.4 RNA Extraction

Chloroform was added to each Trizol sample at a volume of 100µL for each 500µL of Trizol sample. RNA extraction was completed as directed by the Life Technologies Trizol Reagent Total RNA Isolation Reagent Protocol. Following RNA extraction, the RNA samples were quality tested using standard protocols and then frozen at -20°C until qPCR (see Appendix B for quality data). Note that only RIN values over 8 were considered acceptable for processing with qPCR.

5.1.5 qPCR

cDNA was synthesized and PCR was performed using standard protocols (see Appendix A). For PCR analysis, the following primers were used, GAPDH (housekeeping gene), TGFB, VEGFA, HGF, IGF, FGF2, FGF7 and ANGPT1. cDNA preparation yielded a total volume of 20µL; 110 µL RNAse-free H20 was added to each cDNA sample to reach a total volume of 130µL and to allow for 24 five µL samples (three replicates for each of the eight primers).

5.2 Mechanical Modeling

Predicting the mechanical properties of fibrin when the thrombin concentration is changed was completed based on literature which has previously testing fibrin. The data correlation and calculations will be addressed further in the results and discussion section.

Chapter 6. Results and Discussion

6.1 Gene Expression

The results herein are from the H1 LR-MSC line. All other cell lines results can be found in Appendix C.

6.1.1 Compared to Baseline

To quantify the changes in gene expression between baseline (t=0) LR-MSCs to the LR-MSCs placed within the scaffold, RNA was isolated from both batches of cells, and RT-PCR was performed on seven carefully chosen targets plus a GAPDH housekeeping gene. Three graphs show the fold changes from baseline (no scaffold) relative to three scaffold groups, from 1 to 24 hours (**Figures 10 to 12**).

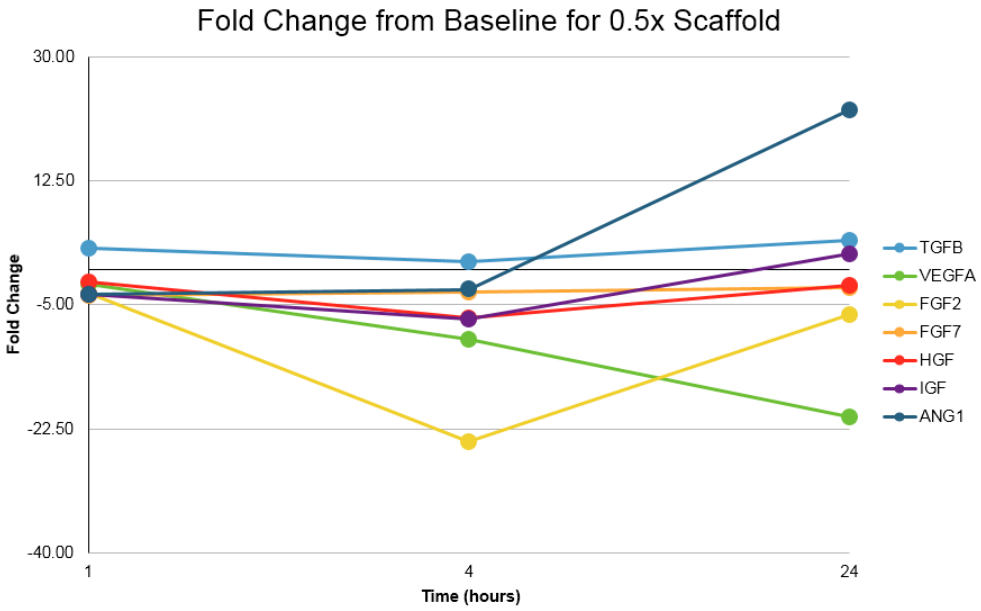

Figure 10. Fold change in gene expression for baseline and 0.5x scaffold group over time.

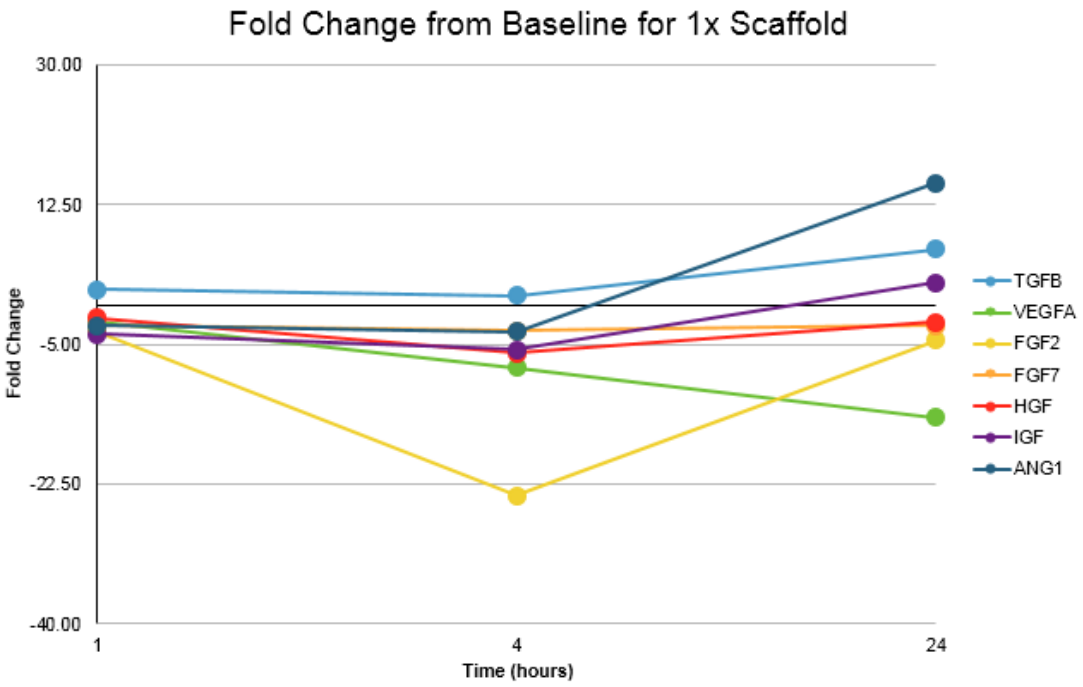

Figure 11. Fold change in gene expression for baseline and 1x scaffold group over time

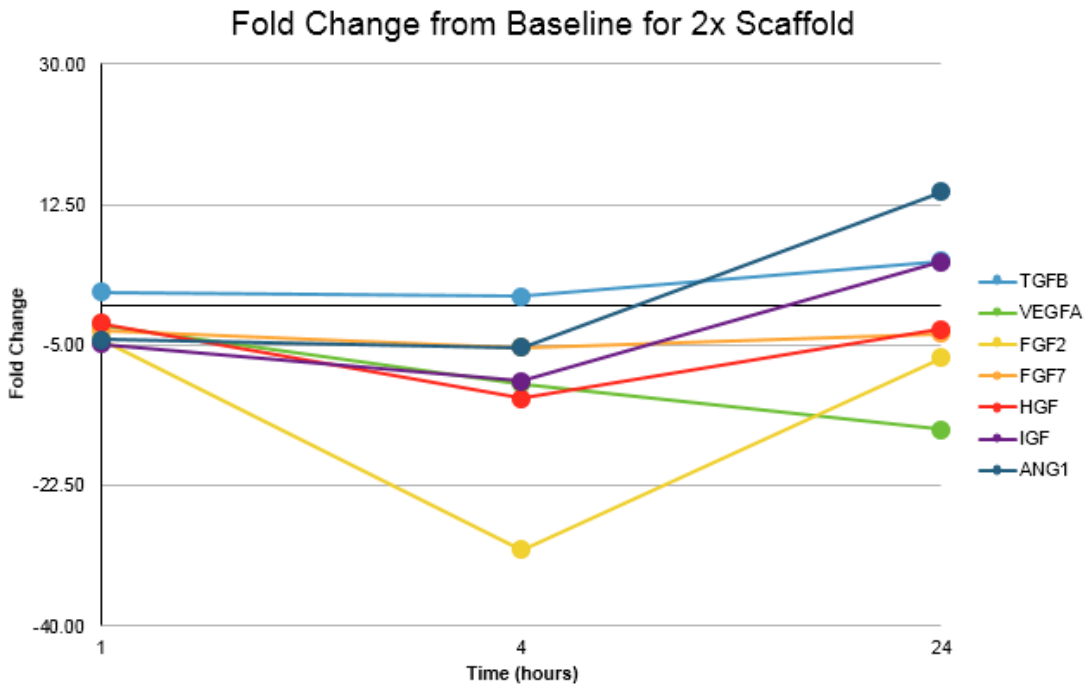

Figure 12. Fold change in gene expression for baseline and 2x scaffold group over time.

For all three scaffolds, FGF-2 showed an apparent decrease in expression at 4 hours, which returns to baseline at 24 hours. TGFB, IGF, and ANG1 showed no major changes from the baseline group at any time tested. All three scaffolds appear to reduce the expression of VEGFA by 24 hours, and appeared to increase the levels of ANG1 by 24 hours.

The fold changes for each sample are shown in **Table 2**. Results are shown only for the changes between the control group of freely suspended cells in media (no scaffold) and the three different scaffold groups. Unfortunately, quality RNA was not obtained for all of the agar control groups so the few agar RNA results will not be discussed here.

Table 2. The fold changes in gene expression relative to the control LR-MSCs freely suspended in media are shown over time at 1, 4 and 24 hours. Targets showing the greatest fold up or down regulation are bolded.

		Fold Change from Control		
Time (hours)	Gene	0.5x Scaffold	1x Scaffold	2x Scaffold
1	TGFB	3.56	2.28	1.97
	VEGFA	2.87	2.64	2.35
	FGF2	-1.20	-1.23	-1.52
	FGF7	-2.59	-1.79	-2.22
	HGF	1.18	1.17	-1.15
	IGF	-1.04	-1.07	-1.41
	ANG1	-2.06	-1.57	-2.57
4	TGFB	2.09	2.06	2.06
	VEGFA	1.85	2.31	1.88
	FGF2	**-**3.12	**-**3.07	**-**3.92
	FGF7	**-**7.16	**-**7.26	**-**11.88
	HGF	-2.81	-2.53	-4.82
	IGF	**-**5.74	**-**4.66	**-**7.73

	ANG1	-3.39	-4.14	-6.36
24	TGFB	3.81	6.41	5.09
	VEGFA	-3.56	-2.41	-2.66
	FGF2	-2.79	-1.97	-2.89
	FGF7	-21.11	-20.97	-29.04
	HGF	-1.83	-1.83	-2.51
	IGF	-2.79	-2.30	-1.16
	ANG1	2.24	1.52	1.40

6.1.2 Compared to Control

To further examine the gene expression within the control and experimental groups at each time point, data from the same experiment in **Figures 13-15** show gene expression at t=1, t=4 and t=24 hours respectively (error bars were not included in the histograms because the standard deviation was very low).

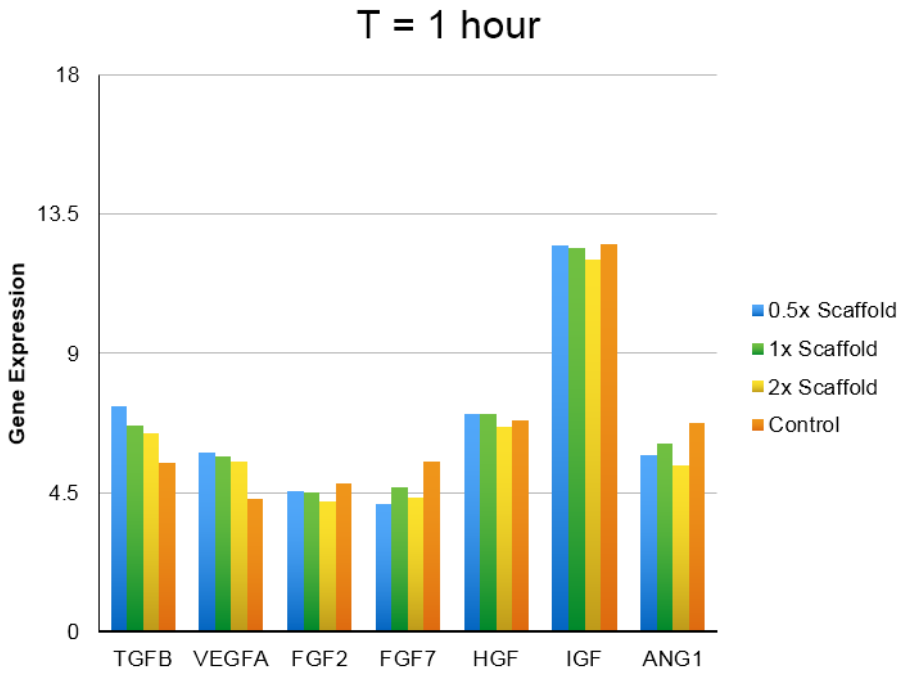

Figure 13. Gene expression at one hour for the control and experimental groups.

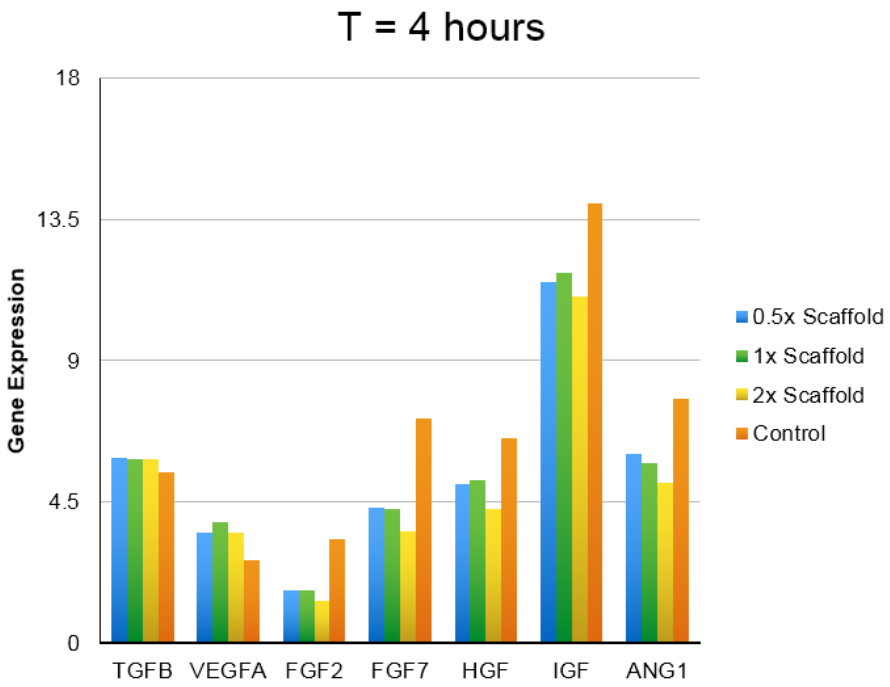

Figure 14. Gene expression at four hours for the control and experimental groups.

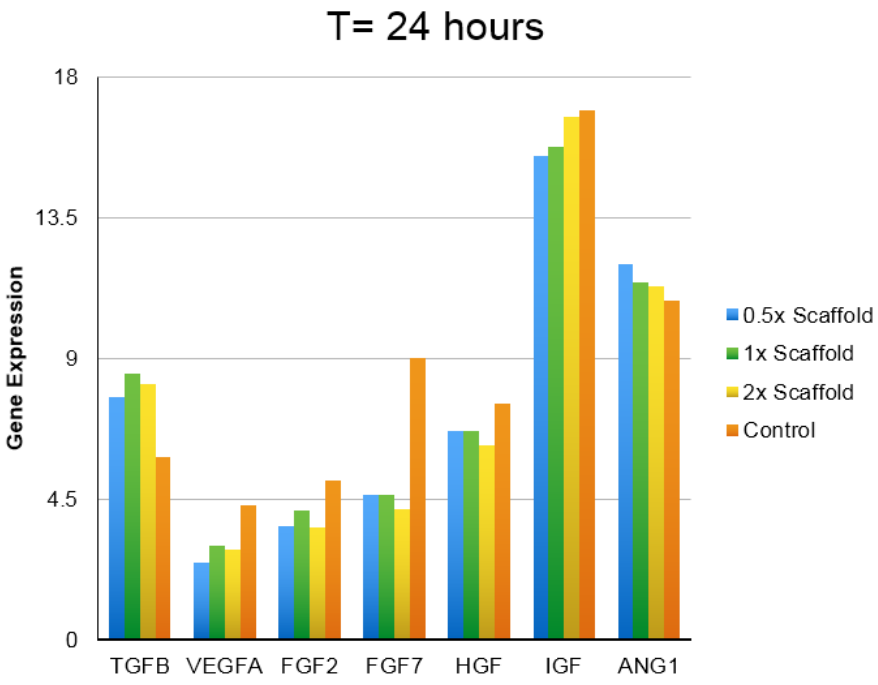

Figure 15. Gene expression at 24 hours for the control and experimental groups.

Figure 15 indicates that of the seven genes assessed for gene expression levels, TGFB and ANG1 in each experimental scaffold are unregulated from the control group after 24 hours. **Figures 13-15** show maintained expression levels of TGFB and increased expression levels of ANG1 overtime, thus ANG1 was chosen as a representative gene for comparing the three scaffold groups.

A statistical analysis was completed to determine whether any of the apparent fold changes from the control were significant for any of the scaffolds at 24 hours (**Table 3**). VEGFA, FGF2, and FGF7 all showed significant changes in gene expression ($p<0.05$) at 24 hours.

Table 3. Statistical significance between three different scaffold groups and the control without scaffold at 24 hours for each gene.

	0.5x	1x	2x
TGFB	**0.0000**	**0.0000**	**0.0004**
VEGFA	**0.0000**	**0.0012**	**0.0001**
FGF2	**0.0003**	**0.0002**	**0.0004**
FGF7	**0.0002**	**0.0001**	**0.0000**
HGF	**0.0017**	**0.0088**	**0.0041**
IGF	**0.0168**	**0.0341**	0.3875
ANG1	**0.0014**	**0.0054**	**0.0007**

Table 3 above does not give statistical differences; however, statistical significance was completed and only showed significant up regulation of TGF-B and ANG1 in the scaffold groups and significant down regulation for all of the remaining genes with the exception of IGF in the 2x scaffold (not bold).

6.1.3 ANG1

Based on the findings in gene expression for baseline and control groups compared to the scaffolds, ANG1 was chosen to further observe changes in the up or down regulation of this gene. To further emphasize the amplitude of change seen in ANG1 over time, **Table 4** below shows the

fold change for each of the six genes compared to ANG1 at 24 hours as well as the statistical difference between gene expression for each gene and ANG1 at 24 hours. Based on this table, it is evident that ANG1 showed a dramatic fold change compared to other genes which showed little change at 24 hours. Furthermore, this is supported by the fact that there is a statistical difference between gene expression for each gene and ANG1 at 24 hours.

Table 4. Fold change between ANG1 and the other genes for the experimental and control group as well as statistical significance between the gene expression of ANG1 and the six other genes at 24 hours.

	Fold Change from ANG1				
	0.5x	**1x**	**2x**	**Control**	**Statistical Difference from ANG1**
TGFB	-18.90	-7.62	-8.88	-32.22	0.007
VEGFA	-744.43	-342.51	-349.71	-93.70	0.001
FGF2	-330.84	-158.68	-215.27	-53.08	0.001
FGF7	-166.57	-112.21	-144.01	-3.53	0.000
HGF	-39.95	-27.10	-34.54	-9.78	0.001
IGF	11.16	19.97	42.81	69.55	0.008

The change in ANG1 expression over time can be seen in **Figure 16** below where the control is cells in media and t=0 is the baseline ANG1 expression.

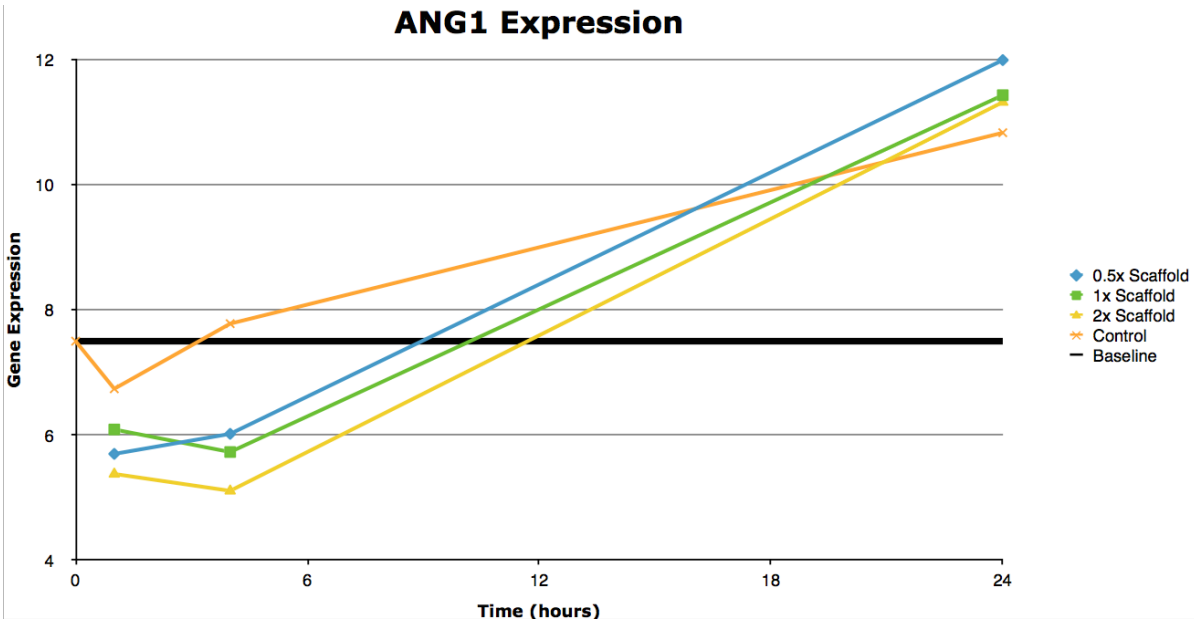

Figure 16. ANG1 expression over time for the baseline, control and experimental groups.

All three of the scaffold groups were significantly unregulated from the baseline group after 24 hours and from the control cells at 24 hours. The 0.5x scaffold showed significant up regulation of ANG1 when compared to the 1x and 2x scaffold groups. With ANG1 as a representative gene that shows unregulated expression levels in the scaffold groups after 24 hours, **Figure 16** implies that the 0.5x scaffold is optimal for this *in vivo* treatment.

6.1.4 Limitations

Unfortunately, the two experimental groups used to evaluate the binding efficiency and effects of cells alone did not result in usable RNA samples. For the H2e cells, very low RNA yields were obtained due to excessive cell binding which indicated that the dextran was not an effective treatment to keep cells in suspension. Likewise, the H8b cells kept in the polypropylene caps had poor recovery, possibly due to the binding of the cells to the caps. Some general observations made throughout experimentation were that at 4 hours and definitely by 24 hours, the cells within the scaffold adopted a typical "MSC" appearance (spreading could be seen as demonstrated in **Figure 8** above). In contrast, the cells within the agarose remained rounded and showed no signs of spreading or obvious migration over the entire experiment. Furthermore, RNA extraction from the agarose gave a lower yield than cells alone or cells within the scaffolds. It is expected that this could possibly be due to agarose binding to the RNA during the extraction or potentially decreased RNA production by the cells themselves.

6.2 Mechanical Modeling

Based on previous research involving the pressures, forces, and elasticity values associated with the lung it was found that the maximum forces in the at total lung capacity are 7.68 N, the maximum pressure is 8 kPa, and the elastic modulus for a single alveolus is approximately 5 kPa

(Hoehm and Marieb, 2013, Suki et al., 2005). In order to determine if the fibrin scaffold is both strong enough and flexible enough to withstand these values, mechanical modeling was done using data from Benkherourou and colleagues. **Figure 17**, below, shows the resulting stress relaxation curve from a 30 μm strain step on a 3 mg/mL fibrin scaffold (Benkerourou, 2000).

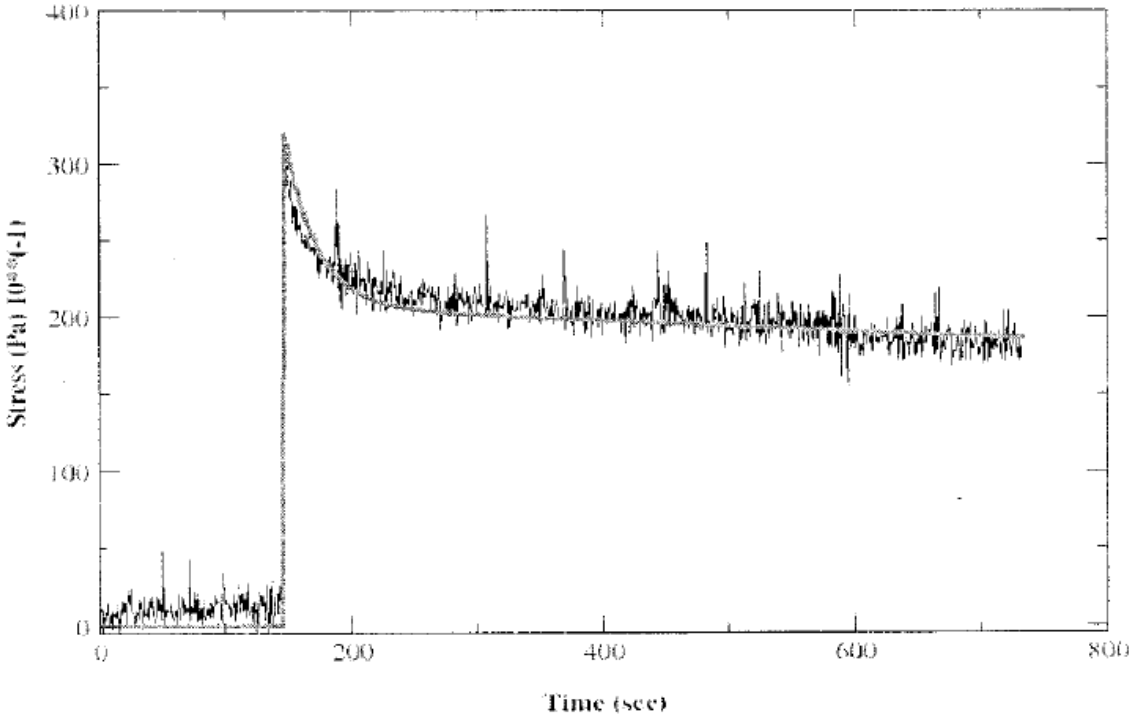

Figure 17. Stress relaxation curve of 3 mg/mL fibrin scaffold as a response to 30 μm step in strain (Benkerourou, 2000).

Using this data and standard linear solid viscoelastic modeling, elastic moduli and the viscosity coefficient of the scaffold could be predicted. The original size of the scaffold in the current study has an area of 9.600 cm^2, therefore, has a diameter of 3.496 cm. According to the definition of strain in Eq. 1, the 30 μm step in strain would cause a strain of 85.81×10^{-3}.

$$\varepsilon = \frac{L - L_o}{L_o} \qquad \text{(Eq. 1)}$$

Where L is equal to the final length after strain (0.03496 m), and L_o is the original length of the specimen (0.03499 m). Therefore the strain percentage change is 0.08581%.

Linear elastic models of a viscoelastic solid are represented by the equation shown in Eq. 2.

$$\sigma(t) = \varepsilon_o \frac{E_1 E_2}{E_1 + E_2}\left[1 + \frac{E_1}{E_2} e^{-\left(\frac{E_1 + E_2}{\eta}\right)t}\right] \qquad \text{(Eq. 2)}$$

Evaluating this relationship when t is equal to 0 seconds, infinity, and a time constant (τ), reveals the elastic moduli (E_1 and E_2) and the viscoelastic constant (η). To first manipulate the relationship, t is equal to 0 seconds. This yields the equation shown in Eq. 3.

$$\sigma(0) = \varepsilon_o \frac{E_1 E_2}{E_1 + E_2}\left[1 + \frac{E_1}{E_2}\right] = \varepsilon_o E_1 \qquad \text{(Eq. 3)}$$

At this point the group was able to solve for E_1, by taking the peak stress from the graph in **Figure 17** to be 32.50 Pa. E_1 was equal to 378.7 Pa.

Taking this value and manipulating Eq. 2 at time equals infinity to reveal Eq. 4 allowed the group to next solve for E_2.

$$\sigma(\infty) = \varepsilon_o \frac{E_1 E_2}{E_1 + E_2} \qquad \text{(Eq. 4)}$$

The stress at time infinity according to the data in **Figure 17** is 20 Pa. This yielded a value of 606.1 Pa for E_2.

Finally, Eq. 2 was manipulated to solve for η. In order to do this the exponential portion of the equation needed to be first set equal to -1 to find the time constant, τ. This first manipulation is shown in Eq. 5.

$$\sigma(\tau) = \varepsilon_o \frac{E_1 E_2}{E_1 + E_2}\left[1 + \frac{E_1}{E_2} e^{-1}\right] \qquad \text{(Eq. 5)}$$

This calculation revealed that at τ, the stress was equal to 24.61 Pa. Referring back to the original data, a value of 24.61 Pa occurs at approximately 200 seconds. Using these values in Eq. 6 revealed the value of the viscosity.

$$\eta = (E_1 + E_2)t \qquad \text{(Eq. 6)}$$

When t is equal to 200 seconds, the viscosity coefficient is equal to 197.0 kPa*s.

After determining the Young's moduli and the viscosity of the original 3 mg/mL fibrinogen scaffold (with 1000 U of thrombin), the group expects that increasing or decreasing thrombin concentration will cause the mechanical properties to change. Since the thrombin concentration will determine the rate at which polymerization occurs and the degree of branching within the polymer, the group predicts that the more thrombin included in the scaffold will result in longer, more intertwined polymers of fibrin. Therefore, more crossing over between polymers will cause more strength in the scaffold. Additionally, since the raw data from Benkherourou et al. (2000) originates from a scaffold from a much smaller size scale, the group predicts that a larger strain

step will also increase the resulting mechanical parameters. Overall, the group predicts that these changes in the scaffold properties would also cause the viscosity coefficient to increase. In order to demonstrate this future rheological testing must be done.

6.3 General Findings

The development of this fibrin scaffold has the potential to influence many individuals as well as populations alike in areas such as health and safety, economics, sustainability, and politics. Overall, the group hopes that since the product is created for the individual's wellbeing, larger scale impacts like global market and economics will be minimal or at least beneficial. In terms of a microeconomic standpoint, the group expects that the scaffold will benefit those with COPD in a sense that they will not have to pay for extensive surgery or life-long medications. The scaffold will allow patients to have one procedure to insert the scaffold into the lungs, and then potentially be on temporary antibiotics in order to ensure no infection occurs due to the surgery. We cannot predict the cost of this regenerative approach at this time but we do expect it will still be costly simply because of the time and complexity involved in deriving LR-MSCs from each individual to create this personalized treatment. However, in the long run, this therapy will better the patient's everyday living because they do not have to worry about future medical bills due to complications or rejection of lung transplants.

On the other hand, the group expects that this scaffold could potentially have a negative effect on political ramifications. While it is expected that this therapy could have potential to be slightly cheaper than a full lung transplant, until the procedure is finalized and made more efficient, there is the distinct possibility that developing countries may not be able to afford the therapy. This impact may also be related to a societal impact in areas that have a middle or lower class economy. The group hopes that after further testing, a more cost efficient method of growing and obtaining

mesenchymal stem cells will allow this therapy to be available for people in a lower income bracket. Furthermore, these implications may also be related to the manufacturability of the product. Fibrin, made of fibrinogen and thrombin, is readily available as well as FDA approved (Evicell by Johnson & Johnson). Therefore, the manufacturing of the actual scaffold should not be problematic. If any problems arise with manufacturing it would be involving the mesenchymal stem cells. This is because the cells not only need to be obtained, but need to be grown substantially as well. This causes the product to be less easily an "off-the-shelf" type of product. More efficient cell growth techniques would need to be developed to decrease the chance of this issue.

In terms of the environment, the overall scope of the project should not have great positive or negative impacts. The scaffold will not be implemented anywhere other than the individual person; therefore, there will not be direct interaction between the environment and this therapy. Likewise, in terms of sustainability, this project would not affect biology or ecology in terms of renewable energy.

Finally, as with any health related products there are ethical considerations and health and safety concerns. Since stem cells are used in conjunction with the developed scaffold, the ethical concern is raised about whether or not stem cells should be used since they are derived from human tissue. In the case of mesenchymal stem cells, they can be developed from any human stromal tissue, therefore we are hoping the availability will limit the ethical concern. Health and safety will likely have positive impacts from the development of this scaffold since the aim of the project is to improve the health of patients with COPD. With using cells as well as a biological scaffold, there is the risk of having a negative immune response. The group hopes that using human derived MSCs will minimize this response. Also, since fibrin is a major component of blood clotting the group hopes that the immune system will not recognize the scaffold as a foreign body.

Chapter 7. Conclusion

Based on the results from gene expression, if the 0.5x scaffold can withstand the mechanical forces seen in the alveoli environment, this scaffold concentration should be explored further to determine whether it is can withstand the dynamic compliance seen in the lung. Although the 0.5x scaffold has shown promise in upregulating ANG1 after 24 hours, increases in mRNA expression do not necessarily correlate with an increase of functional protein release; therefore, future studies using transwells to observe protein release through the scaffold to a secondary cell line need to be done. Finally, to validate the mechanical modeling, rheology should be used to test various fibrin scaffolds with and without cells.

Chapter 8. Future Recommendations

Although the study showed promising results regarding the potential for this therapy *in vivo*, additional testing should be completed. To validate whether changes in gene expression resulted in functional protein release, a test method for using transwells to see the potency effect of LR-MSCs within scaffold groups on a secondary cell line such as endothelial cells would be useful. This type of proposed system can be seen in **Figure 18**.

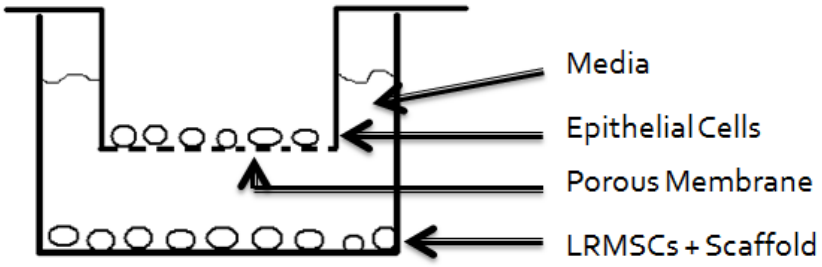

Figure 18. The transwell set-up using two separated cell lines with a reservoir of media to nourish the cells and allow for exchange of extracellular vesicles or signals. The porous membrane should be optimized to allow for signal exchange but not for cell migration.

Analysis of the secondary cell line in terms of viability and proliferation should be completed to determine whether the changes in gene expression of LR-MSCs have a strong influence on the fate of endothelial cells. Ideally, the growth factors should promote endothelial cell survival and proliferation. Alternative studies simply using western blots to analyze protein release from the scaffold with cells could also be completed.

In order to demonstrate the group's prediction about the effect of thrombin on mechanical properties of the scaffold, the group would continue testing through rheology. Based on a study by Wedgwood (2013), stress amplitude tests and frequency sweep tests would be combined to obtain more accurate values of the mechanical parameters outlined in the mechanical modeling section (Wedgwood, 2013). Through this testing, the group would expect to obtain additional parameters

such as the loss modulus, storage modulus, and complex viscosity. Based off of the results of this testing, it is predicted that these mechanical parameters will be able to more accurately match the scaffold with a viscosity model, while also showing the relationship between viscosity and thrombin concentration. Furthermore, knowing these relationships, the group expects to better validate the composition of the final scaffold.

References

Ahlfors, JW & Billiar, KL. (2007). Biomechanical and biochemical characteristics of a human fibroblast-produced and remodeled matrix. *Biomaterials*. 28: 2183-2191.

Assoian RK, Fleurdelys BE, Stevenson HC, Miller PJ, Madtes DK, Raines EW, Ross R, and Sporn MB (1987) "Expression and secretion of type β transforming growth factor by activated human macrophages. *Proc. Natl. Acad. Sci. USA*, 84: 6020.

Benkherourou M, et al. (2000) Quantification and Macroscopic Modeling of the Nonlinear Viscoelastic Behavior of Strained Gels with Varying Fibrin Concentrations. *IEEE Transactions on Biomedical Engineering*, 47: 1465-1475.

Boriello G, Goel M, Heltshe S, Larson E & Patel S (2012) SpiroSmart: Using a microphone to measure lung function on a mobile phone. Retrieved September 20, 2013, from https://dl.dropbox.com/u/6183880/SpiroSmart.CR.Final.pdf.

Breen EC (2007) VEGF in biological control. *J Cell Biochem*,102: 1358–1367.

Brown AC, & Barker TH (2014) Fibrin-based biomaterials: Modulation of macroscopic properties through rational design at the molecular level. *Acta Biomaterialia, 10*(4): 1502-1514.

CDC/National Center for Health Statistics (2013) *Chronic Obstructive Pulmonary Disease (COPD) Includes: Chronic Bronchitis and Emphysema*. Retrieved from http://www.cdc.gov/nchs/fastats/copd.htm

Chantry D, et al. (1989) "Modulation of Cytokin Production by Transforming Growth Factor-β1". *The Journal of Immunology*, 142: 4295-4300.

Collins J, Thebaud B (2013) Lung mesenchymal stromal cells in development and disease: to serve and protect? Sprott Centre for Stem Cell Research, 2013.

Dailey L, Ambrosetti D, Mansukhani A, & Basilico C (2005) Mechanisms underlying differential responses to FGF signaling. *Cytokine & Growth Factor Reviews, 16*(2): 233-247.

Davis AM, Hoffman AM, Ingenito EP, Mazan MR, Murthy S, Paxson JA, & Tyagi S (2011) Lung-derived mesenchymal stromal cell post-transplantation survival, persistence, paracrine expression, and repair of elastase-injured lung. *Stem Cells and Development, 20*, 1779-1792.

Ellingsworth LR, et al. (1988) "Transforming growth factor-βs are equipotent growth inhibitors of interleukin 1 induced thymocyte proliferation." *Cellular Immunology*, 114: 41.

Epidemiology and Statistics Unit, American Lung Association (2012) *Estimated prevalence and incidence of lung disease*. Retrieved from http://www.lung.org/finding---cures/our---research/trend---reports/estimated---prevalence.pdf

Fitzgerald KA, O'Neill LAJ, & Gearing AJH (2001) *Cytokine factsbook and webfacts*. London, GBR: Academic Press.

Hoehm EN & Marieb K (2013) *Human Anatomy and Physiology* (Ninth Edition). Glenview, IL: Pearson Education.

Huang, NF et al. (2010). Biophysical and chemical effects of fibrin on mesenchymal stromal cell gene expression. *Acta Biomaterialia*. 6: 3947-3956.

Ingenito, E. P. (2010). Aeirs Therapeutics (Ed.), *Tissue volume reduction* (604/514). Kingston/MA: A61M31/00. Retrieved from http://www.google.com.ar/patents/US7654998.

Ingenito EP, Tyagi S, Tsal L, Hoffman A (2012) "Autologous Lung Multipotent Stromal Cell Therapy for Emphysema." A Grant Proposal.

Kehrl JH, Roberts AB, Wakefield LM, Jakowlew S, Sporn MB, and Fauci AS. (1986a) "Transforming growth factor β is an important immunomodulatory protein for human B lymphocytes. *Journal of Immunology*, 137: 3855.

Kehrl JH and Wakefield LM, et al. (1986b) "Production of transforming growth factor β by human T lymphocytes and its potential role in the regulation of T cell growth. *Journal of Experimental Medicine,* 163: 1037.

Koh GY (2013) Orchestral actions of angiopoietin-1 in vascular regeneration. *Trends in Molecular Medicine, 19*(1): 31-39.

Laron Z (2001) Insulin-like growth factor 1 (IGF-1): a growth hormone. *Molecular Pathology,* 54: 311-316.

Linnes, MP; Ratner, BD; & Giachelli, CM. (2007) A fibrinogen-based precision microporous scaffold for tissue engineering. *Biomaterials*. 28: 5298-5306.

Matsumoto K, Nakamura T (1996) "Emerging Multipotent Aspects of Hepatocyte Growth Factor." *Journal of Biochemistry,* 119: 591-600.

Mijailovich SM, et al. (1994) "Dynamic moduli of rabbit lung tissue and pigeon ligamentum propatagiale undergoing uniaxial cyclic loading." *The American Physiological Society,* 94: 773-782.

Neuss S, Becher E, Woltje M, Tietze L, Jahnen-Dechent W (2004) "Functional Expression of HGF and HGF Receptor/c-met in Adult Human Mesenchymal Stem Cells Suggests a

Role in Cell Mobilization, Tissure Repair, and Wound Healing." *Stem Cells,* 22: 405-414.

Ogunwobi OO, Puszyk W, Dong HJ, Liu C (2013) "Epigenetic Upregulation of HGF and c-Met Drives Metastasis in Hepatocellular Carcinoma." *PLoS ONE,* 8: e63765.

Pribylova-Hribova P, Kotsch K, Lodererova A, Viklicky O, Vitko S, Volk HD, and Lacha J (2006) "TGF-β1 mRNA upregulation influences chronic renal allograft dysfunction." *Kidney International,* 69: 1872-1879.

Puente P, & Ludeña D (2014) Cell culture in autologous fibrin scaffolds for applications in tissue engineering. *Experimental Cell Research, 322*(1): 1-11.

Ranges GE, Figari IS, Espevik T, and Paladino MA (1987) "Inhibition of cytotoxic T cell development by transforming growth factor β and reversal by recombinant tumor necrosis factor a." *J. Exp. Med.* 166: 991.

Rhoades R, Bell D (2009) *Medical Physiology: Principles of Clinical Medicine*. (Third ed.) Baltimore, MD: Lippincott Williams & Wilkins.

Ricciardi M, Malpeli G, Bifari F, Bassi G, Pacelli L, et al. (2012) Comparison of Epithelial Differentiation and Immune Regulatory Properties of Mesenchymal Stromal Cells Derived from Human Lung and Bone Marrow. doi:10.1371/journal.pone.0035639

Rook AH, et al. (1986) "Effects of transforming growth factor β on the functions of natural killer cells: Depressed cytolytic activity and blunting of interferon responsiveness. *Journal of Immunology,* 136: 3916.

Schleede S, Meinel FG, Bech M, et al. (2012) "Emphysema diagnosis using X-ray dark-field imaging at a laser-driven compact synchrotron light source." Proc Natl Acad Sci USA, 109(44): 17880–17885.

Shalaby MR, Ammann AJ (1988) "Suppression of immune cell function *in vitro* by recombinant human transforming growth factor-β. *Cell. Immunol.* 112: 343.

Stewart, CE & Rotwein P (1996) Growth, Differentiation, and Sruvival: Multiple Physiological Functions for Insulin-Like Growth Factors. *Physiological Reviews, 76:* 1005-1026.

Suki B, et al. (2005) "Biomechanics of the lung parenchyma: critical roles of collagen and mechanical forces." *Journal of Applied Physiology,* 98: 1892-1899.

Swartout-Corbeil D, Skinner P, & Frey RJ (2011) Emphysema. In L. J. Fundukian (Ed.), *The Gale Encyclopedia of Medicine* (4th ed. ed., pp. 1523-1530). Detroit: Gale.

"The Respiratory System" (2012) National Heart, Lung, and Blood Institute. Retrieved from http://www.nhlbi.nih.gov/health/health-topics/topics/hlw/system.html.

Townsend MC (2011) “Spirometry in the occupational health setting.” *Journal of occupational and environmental medicine/American College of Occupational and Environmental Medicine,* 53: 5.

Veikkola T, & Alitalo K (1999) VEGFs, receptors and angiogenesis. *Seminars in Cancer Biology*, *9*(3): 211-220.

Wedgwood, J., Freemont, A. J., & Tirelli, N. (2013). Rheological and turbidity study of fibrin h ydrogels. *Macromolecular Symposia, 334*(1), 117-125. doi:10.1002/masy.201300111

Weiss D: Mesenchymal stem cells for lung repair and regeneration. University of Vermont College of Medicine, 2010.

Appendix A: Protocols

qRT-PCR (RT2 SYBER Green Mastermix)

1. Need 5 uL of cDNA per reaction so enough RNAse free water was added to ensure that there was enough cDNA for the reaction
2. Reaction mix (per sample):
   RT Mastermix: 12.5 uL
   Water: 6.5 uL
   Primer Mix (10 uM each): 1 uL
3. Add 20 uL of the reaction mix to each sample with 5 uL of the cDNA to reach a total volume of 25uL reaction volume
4. Add either caps or tape to seal plate
5. Spin PCR plate down briefly before placing into machine for analysis
6. Place into machine for analysis

Appendix B: RNA Quality

Table 5. RNA quality for H1 cell line. Although RIN values were not retrieved for rows 8-10 and the quality for rows 14 & 15 was 7.7, the samples were still processed using qPCR and gene expression was seen.

H1		RIN	Conc (ng/uL)	RNA (1000ng)	H_2O
1	T0 cells	8.8	470	2.1	5.9
2	T1 cells	8.8	417	2.4	5.6
3	T1 S0.5x	8.7	306	3.3	4.7
4	T1 S1x	8.8	351	2.8	5.2
5	T1 S2x	8.6	328	3.0	5.0
6	T1 Ag	9.2	76	-	-
7	T4 cells	8.7	529	1.9	6.1
8	T4 S0.5x	-	377	2.7	5.3
9	T4 S1x	-	333	3.0	5.0
10	T4 S2x	-	305	3.3	4.7
11	T4 Ag	9.6	205	4.9	3.1
12	T24 cells	8.1	147	6.8	1.2
13	T24 S0.5x	8.0	146	6.8	1.1
14	T24 S1x	7.7	145	6.9	1.1
15	T24 S2x	7.7	158	6.3	1.7
16	T24 Ag	9.2	73	-	-
17	T48 cells	4.2	20	-	-
18	T48 S0.5x	8.1	107	-	-
1	T48 S1x	7.6	147	6.8	1.2
20	T48 S2x	7.8	81	-	-
21	T48 Ag	8.1	32	-	-

Table 6. RNA quality for H2 cell line. Note that the cells w/d stands for the control group of cells on plates coated with dextran.

H2		RIN	Conc (ng/uL)	RNA (1000ng)	H_2O
1	T0 cells	9.3	423	2.4	5.6
2	T1 cells	9.1	371	2.7	5.3
3	T1 cells w/d	-	9	-	-
4	T1 S0.5x	9.8	265	3.8	4.2
5	T1 S1x	9.7	256	3.9	4.1
6	T1 S2x	9.5	309	3.2	4.8
7	T1 Ag	9.7	144	6.9	1.1
8	T4 cells	9.0	370	2.7	5.3
9	T4 cells w/ d	8.4	28	-	-
10	T4 S0.5x	9.4	286	3.5	4.5
11	T4 S1x	9.6	316	3.2	4.8
12	T4 S2x	9.3	268	3.7	4.3
13	T4 Ag	9.4	203	4.9	3.1
14	T24 cells	8.8	388	2.6	5.4
15	T24 cells w/ d	9.0	155	6.5	1.5
16	T24 S0.5x	-	247	4.0	4.0
17	T24 S1x	-	167	6.0	2.0
18	T24 S2x	-	151	6.6	1.4

1	T24 Ag	9.1	55	-	-
20	T48 cells	4.4	46	-	-
21	T48 cells w/ d	4.4	18	-	-
22	T48 S0.5x	6.9	133	7.5	0.5
23	T48 S1x	7.3	76	-	-
24	T48 S2x	8.7	144	6.9	1.1
25	T48 Ag	-	5	-	-

Table 7. RNA quality for H4 cell line.

H4		RIN	Conc (ng/uL)	RNA (1000ng)	H_2O
1	T0 cells	9.9	468	2.1	5.9
2	T1 cells	9.7	488	2.0	6.0
3	T1 S0.5x	10	278	3.6	4.4
4	T1 S1x	10	523	1.9	6.1
5	T1 S2x	9.9	331	3.0	5.0
6	T1 Ag	9.7	15	-	-
7	T4 cells	9.5	566	1.8	6.2
8	T4 S0.5x	10	405	2.5	5.5
9	T4 S1x	9.9	397	2.5	5.5
10	T4 S2x	10	325	3.1	4.9
11	T4 Ag	9.7	20	-	-
12	T24 cells	9.1	302	3.3	4.7
13	T24 S0.5x	-	235	4.3	3.7
14	T24 S1x	-	86	-	-
15	T24 S2x	-	296	3.4	4.6
16	T24 Ag	9.9	33	-	-
17	T48 cells	4.9	40	-	-
18	T48 S0.5x	-	442	2.3	5.7
19	T48 S1x	-	356	2.8	5.2
20	T48 S2x	-	148	6.8	1.2
21	T48 Ag	-	10	-	-

Table 8. RNA quality for H8 cell line

H8		RIN	Conc (ng/uL)	RNA (1000ng)	H_2O
1	T0 cells	9.3	710	1.4	6.6
2	T1 S0.5x	10	681	1.5	6.5
3	T1 S1x	10	741	1.3	6.7
4	T1 S2x	10	775	1.3	6.7
5	T1 Ag	9.6	489	2.0	6.0
6	T4 S0.5x	9.2	686	1.5	6.5
7	T4 S1x	9.5	587	1.7	6.3
8	T4 S2x	-	297	3.4	4.6
9	T4 Ag	9.7	260	3.8	4.2
10	T24 S0.5x	-	219	4.6	3.4
11	T24 S1x	-	384	2.6	5.4
12	T24 S2x	-	289	3.5	4.5

13	T24 Ag	9.5	86	-	-

Table 9. RNA quality for H8b cell line. Note that the "cells cap" groups were the control groups cultured on the polypropylene caps.

H8b		RIN	Conc (ng/uL)	RNA (1000ng)	H_2O
1	T0 cells	9.3	371	2.7	5.3
2	T1 cells	9.3	352	2.8	5.2
3	T1 cells cap	-	18	-	-
4	T1 S0.5x	9.7	188	5.3	2.7
5	T1 S1x	9.7	214	4.7	3.3
6	T1 S2x	9.5	223	4.5	3.5
7	T1 Ag	9.8	156	6.4	1.6
8	T4 cells	9.0	332	3.0	5.0
9	T4 cells cap	-	3	-	-
10	T4 S0.5x	9.8	174	5.7	2.3
11	T4 S1x	9.9	182	5.5	2.5
12	T4 S2x	9.9	318	3.2	4.8
13	T4 Ag	9.3	226	4.4	3.6
14	T24 cells	8.7	186	5.4	2.6
15	T24 cells cap	-	4	-	-
16	T24 0.5x	-	125	8.0	0.0
17	T24 S1x	-	106	-	-
18	T24 S2x	-	132	7.6	0.4
19	T24 Ag	9.4	28	-	-

Appendix C: Gene Expression Results

H2

Compared to Baseline

Table 10. H2 cells: Statistical significance of gene expression between each scaffold group and the baseline for each gene.

	0.5x	1x	2x
TGFB	0.378	0.329	0.463
VEGFA	0.025	0.068	0.036
FGF2	0.131	0.215	0.126
FGF7	0.270	0.455	0.211
HGF	0.126	0.284	0.128
IGF	0.210	0.151	0.217
ANG1	0.240	0.173	0.196

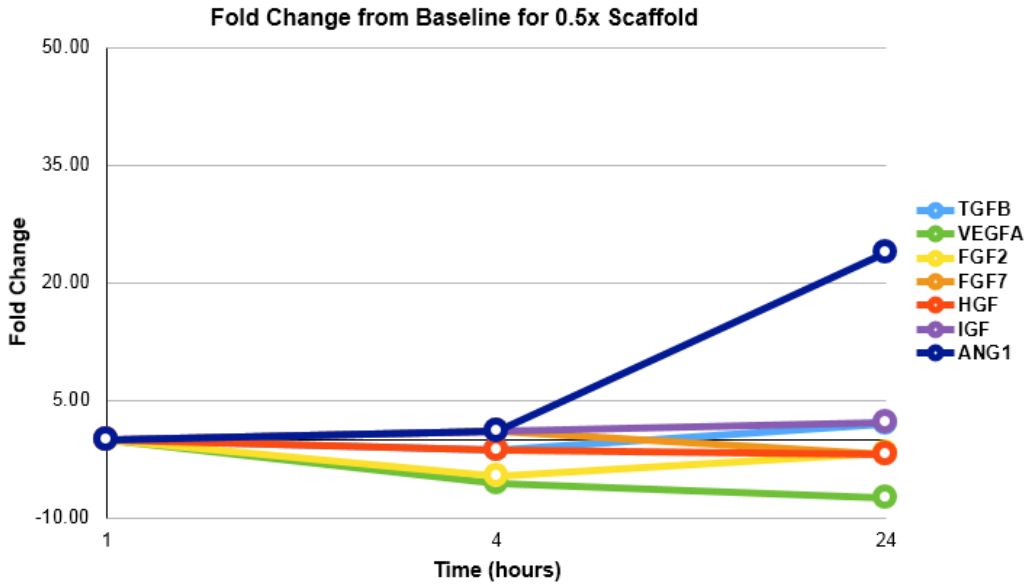

Figure 19. Fold change in gene expression of H2 cells for baseline and 0.5x scaffold group over time.

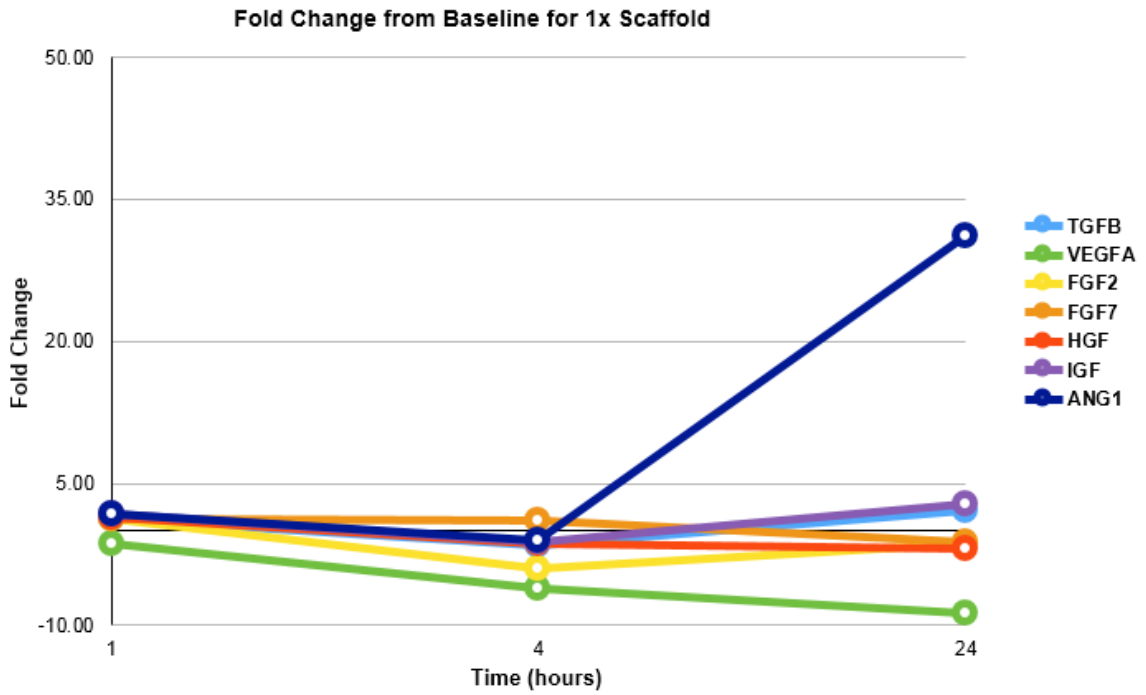

Figure 20. Fold change in gene expression of H2 cells for baseline and 1x scaffold group over time.

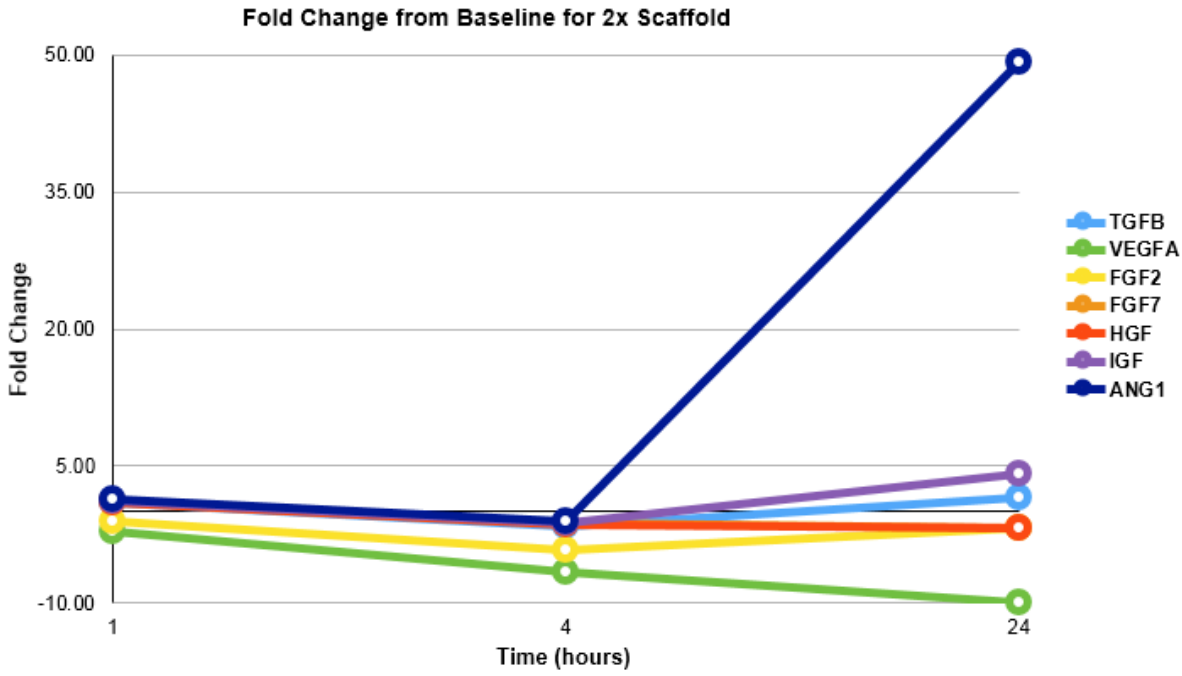

Figure 21. Fold change in gene expression of H2 cells for baseline and 2x scaffold group over time.

Compared to Control

Table 11. The fold changes in gene expression relative to the control H2 LR-MSCs freely suspended in media are shown over time at 1, 4 and 24 hours.

		Fold Change from Control		
Time (hours)	**Gene**	**0.5x Scaffold**	**1x Scaffold**	**2x Scaffold**
1	**TGFB**	n/a	1.61	1.40
	VEGFA	n/a	2.30	1.43
	FGF2	n/a	-1.80	-2.33
	FGF7	n/a	-2.19	-2.43
	HGF	n/a	-1.49	-2.10
	IGF	n/a	-2.57	-3.41
	ANG1	n/a	-1.83	-2.41
4	**TGFB**	1.43	1.23	1.24
	VEGFA	1.02	-1.05	-1.14
	FGF2	-2.85	-2.41	-2.62
	FGF7	-4.63	-4.72	-6.06
	HGF	-2.64	-2.89	-2.81
	IGF	-7.94	-10.06	-10.93
	ANG1	-4.17	-4.76	-4.82
24	**TGFB**	2.45	2.68	1.97
	VEGFA	-2.16	-2.48	-2.83
	FGF2	-4.66	-3.39	-4.47
	FGF7	-27.47	-17.75	-25.81
	HGF	-10.20	-9.65	-9.58
	IGF	-23.26	-17.39	-11.71
	ANG1	-2.66	-2.03	-1.28

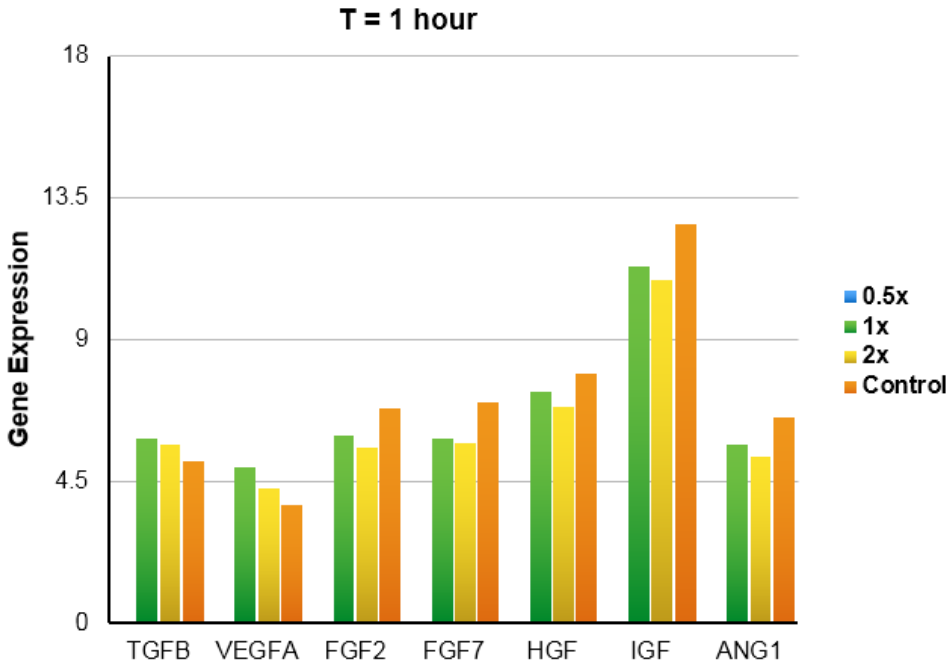

Figure 22. Gene expression at one hour for the experimental groups for H2 cell line. Note that quality RNA could not be achieved for the control group.

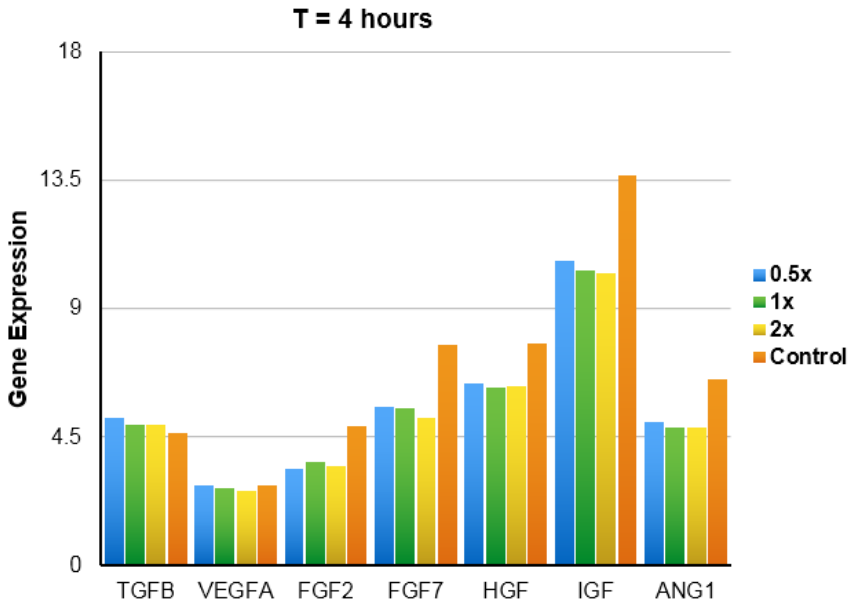

Figure 23. Gene expression at four hours for the control and experimental groups for H2 cell line.

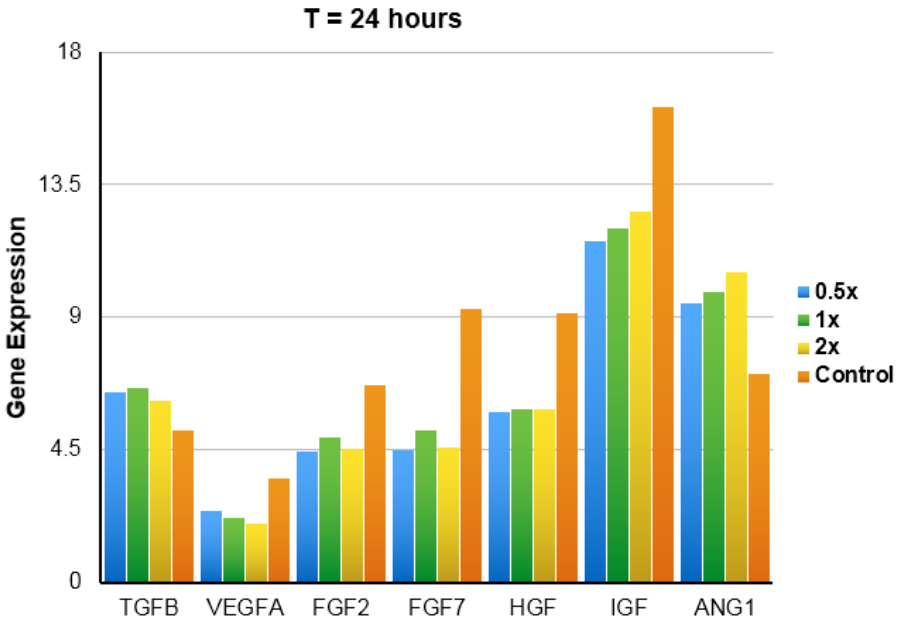

Figure 24. Gene expression at 24 hours for the control and experimental groups for H2 cell line.

H4

Compared to Baseline

Table 12. H4 cells: Statistical significance of gene expression between each scaffold group and the baseline for each gene.

	0.5x	1x	2x
TGFB	0.150	0.056	0.145
VEGFA	0.095	0.163	0.115
FGF2	0.050	0.140	0.077
FGF7	0.128	0.219	0.049
HGF	0.077	0.112	0.061
IGF	0.297	0.037	0.099
ANG1	0.352	0.415	0.224

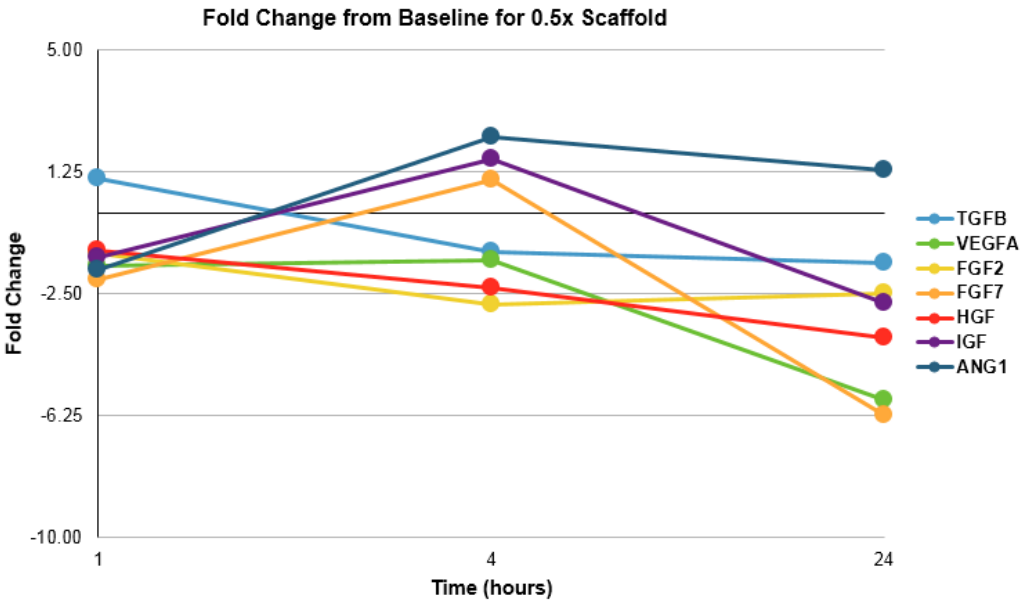

Figure 25. Fold change in gene expression of H4 cells for baseline and 0.5x scaffold group over time.

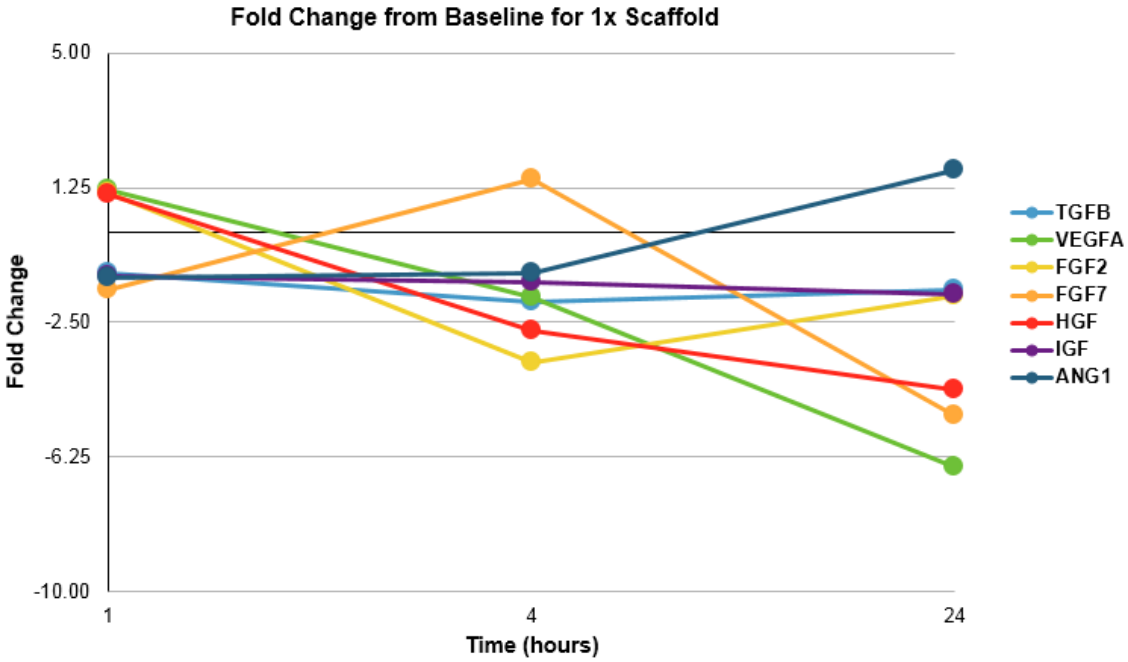

Figure 26. Fold change in gene expression of H4 cells for baseline and 1x scaffold group over time.

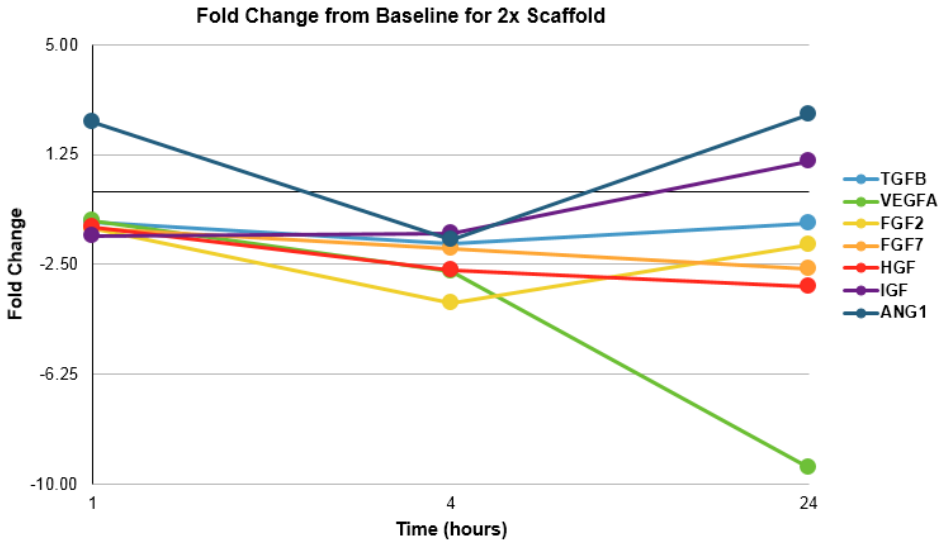

Figure 27. Fold change in gene expression of H4 cells for baseline and 2x scaffold group over time.

Compared to Control

Table 13. The fold changes in gene expression relative to the control H4 LR-MSCs freely suspended in media are shown over time at 1, 4 and 24 hours.

		Fold Change from Control		
Time (hours)	Gene	0.5x Scaffold	1x Scaffold	2x Scaffold
1	TGFB	1.79	1.51	1.65
	VEGFA	1.22	2.31	1.92
	FGF2	-1.78	-1.27	-1.78
	FGF7	-2.35	-1.83	-1.45
	HGF	-1.32	-1.05	-1.37
	IGF	-1.66	-1.48	-1.87
	ANG1	-2.11	-1.53	1.97
4	TGFB	1.91	1.18	1.28
	VEGFA	3.73	2.99	1.97
	FGF2	-2.93	-3.73	-3.94
	FGF7	-3.12	-2.11	-6.15
	HGF	-1.21	-1.43	-1.41
	IGF	-2.13	-4.86	-5.13
	ANG1	1.11	-2.39	-3.48
24	TGFB	1.38	1.33	1.92
	VEGFA	-2.38	-2.69	-3.89
	FGF2	-13.18	-9.38	-9.71
	FGF7	-56.89	-46.53	-24.08
	HGF	-10.93	-12.38	-9.19
	IGF	-73.52	-45.89	-26.17
	ANG1	-19.97	-14.93	-9.85

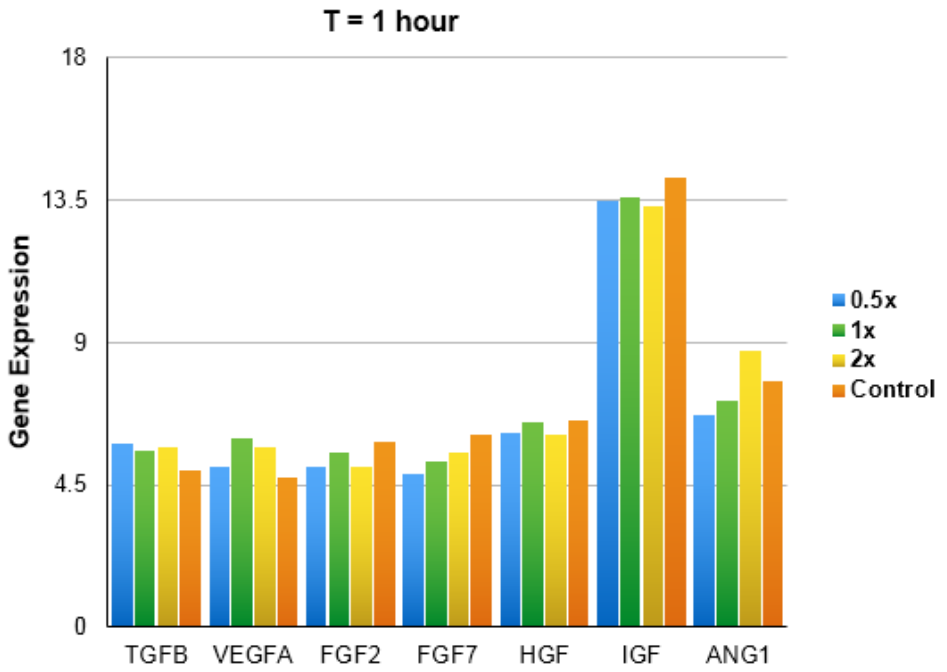

Figure 28. Gene expression at one hour for the control and experimental groups for H4 cell lines.

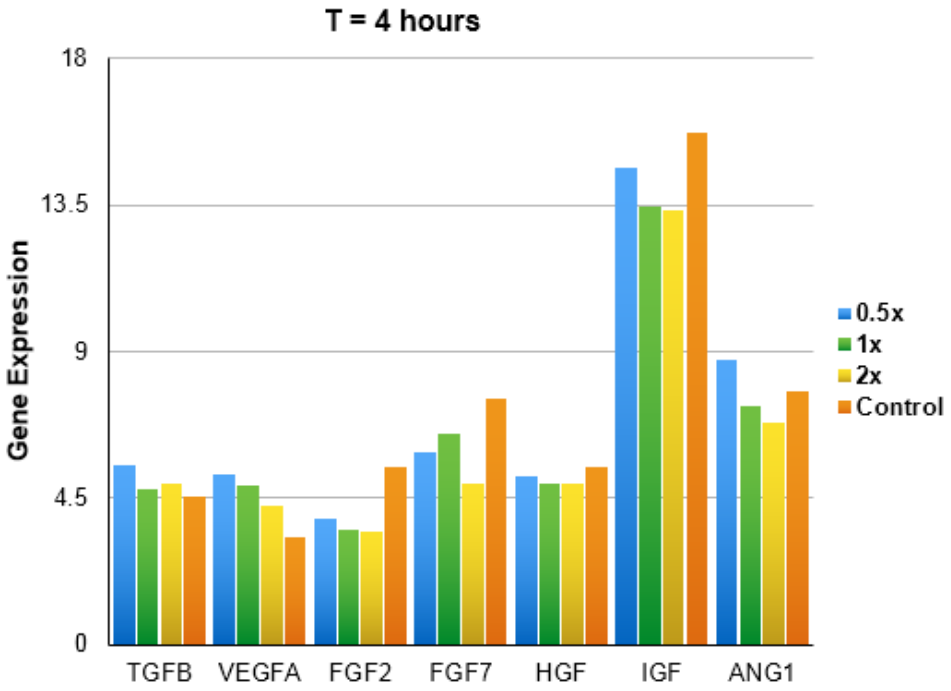

Figure 29. Gene expression at four hours for the control and experimental groups for H4 cell line.

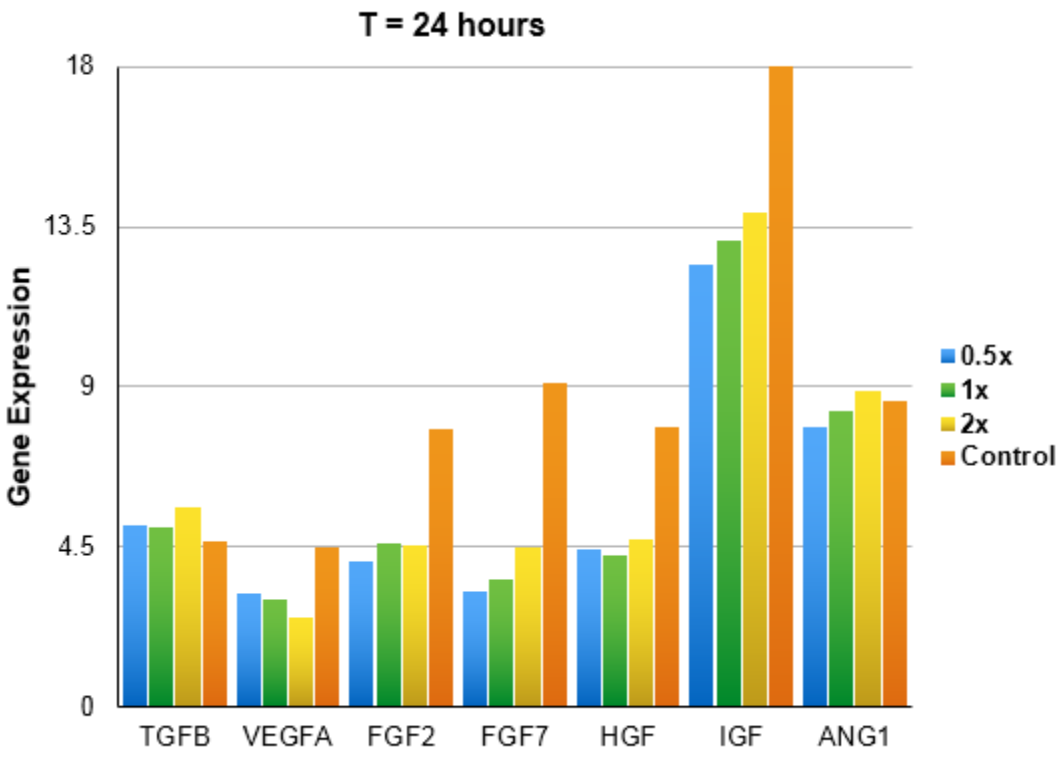

Figure 30. Gene expression at 24 hours for the control and experimental groups for H4 cell line.

H8

Compared to Baseline

Table 14. H8 cells: Statistical significance of gene expression between each scaffold group and the baseline for each gene.

	0.5x	1x	2x
TGFB	0.091	0.029	0.019
VEGFA	0.017	0.025	0.019
FGF2	0.016	0.015	0.015
FGF7	0.001	0.004	0.005
HGF	0.011	0.020	0.018
IGF	0.029	0.011	0.017
ANG1	0.104	0.094	0.114

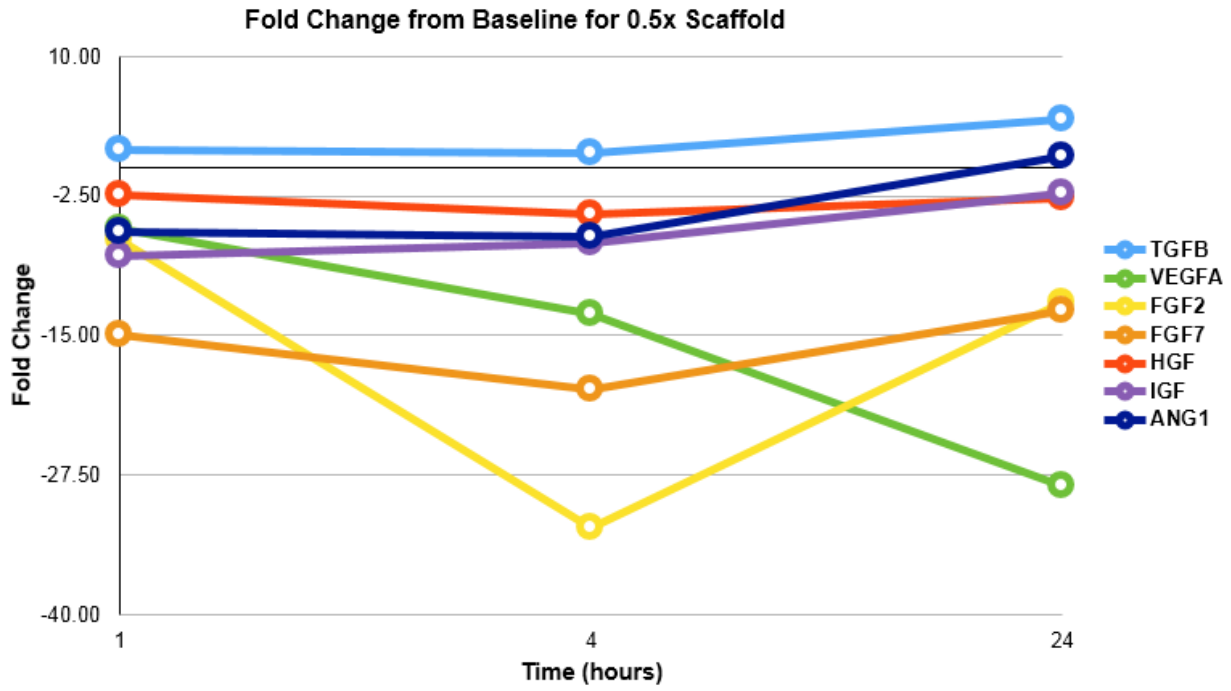

Figure 31. Fold change in gene expression of H8 cells for baseline and 0.5x scaffold group over time.

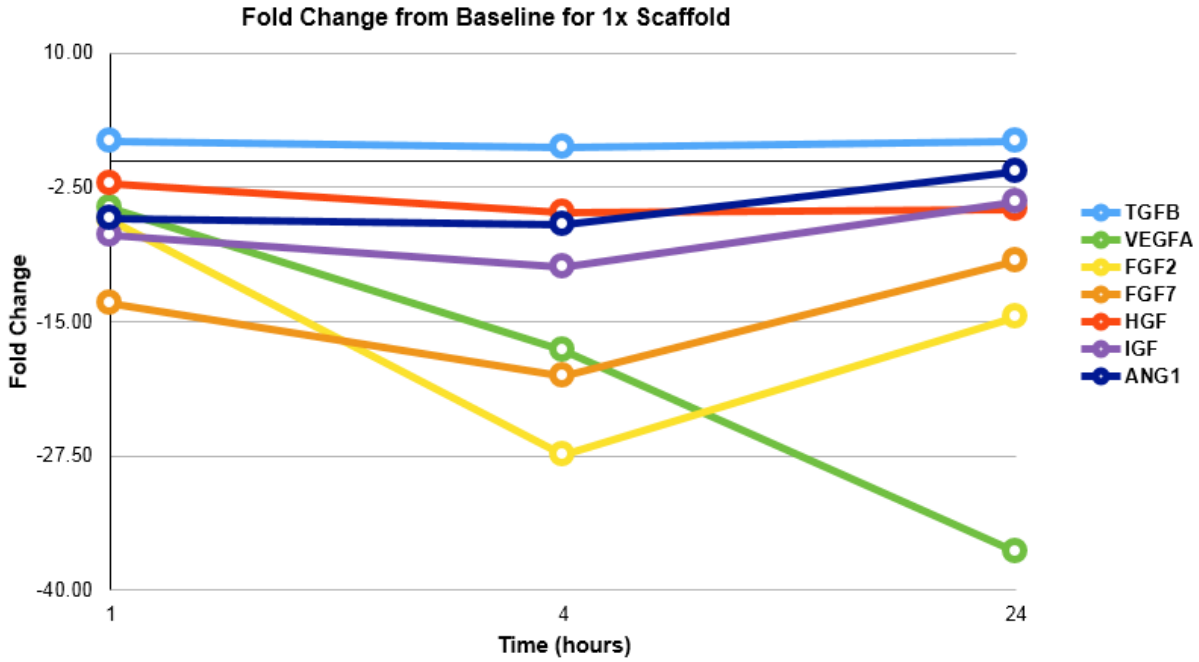

Figure 32. Fold change in gene expression of H8 cells for baseline and 1x scaffold group over time

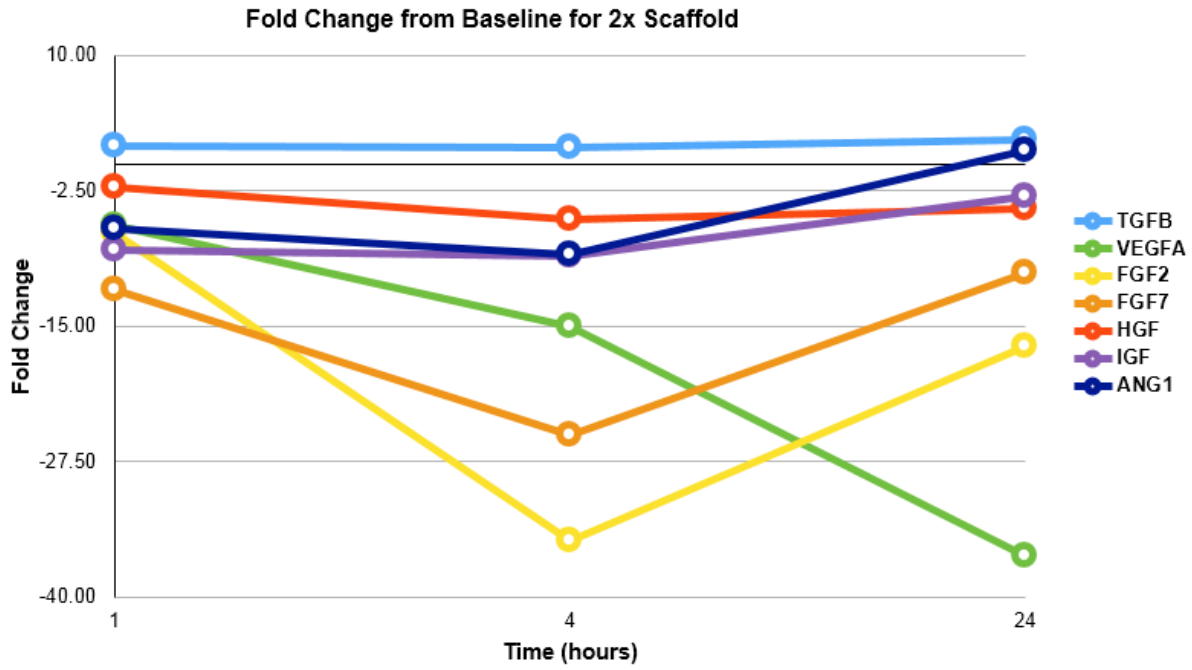

Figure 33. Fold change in gene expression of H8 cells for baseline and 2x scaffold group over time

Compared to Control

RNA could not be retrieved from the control groups because there were not enough cells left to run the experiments which resulted in the inability to get quality mRNA.

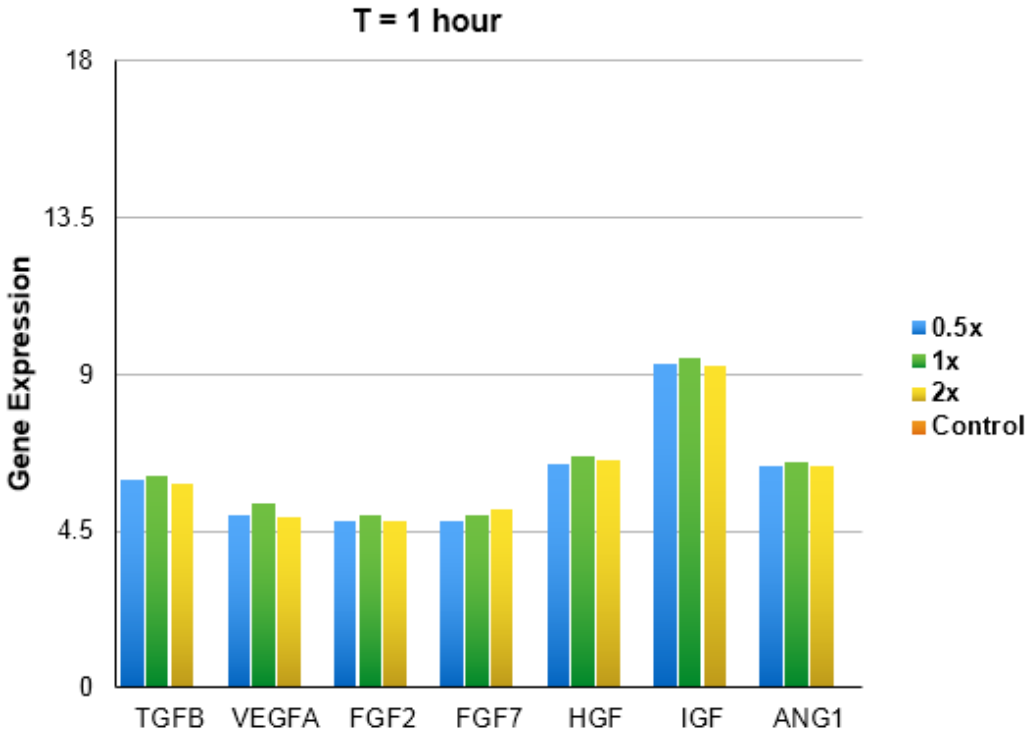

Figure 34. Gene expression at one hour for the control and experimental groups for H4 cell line.

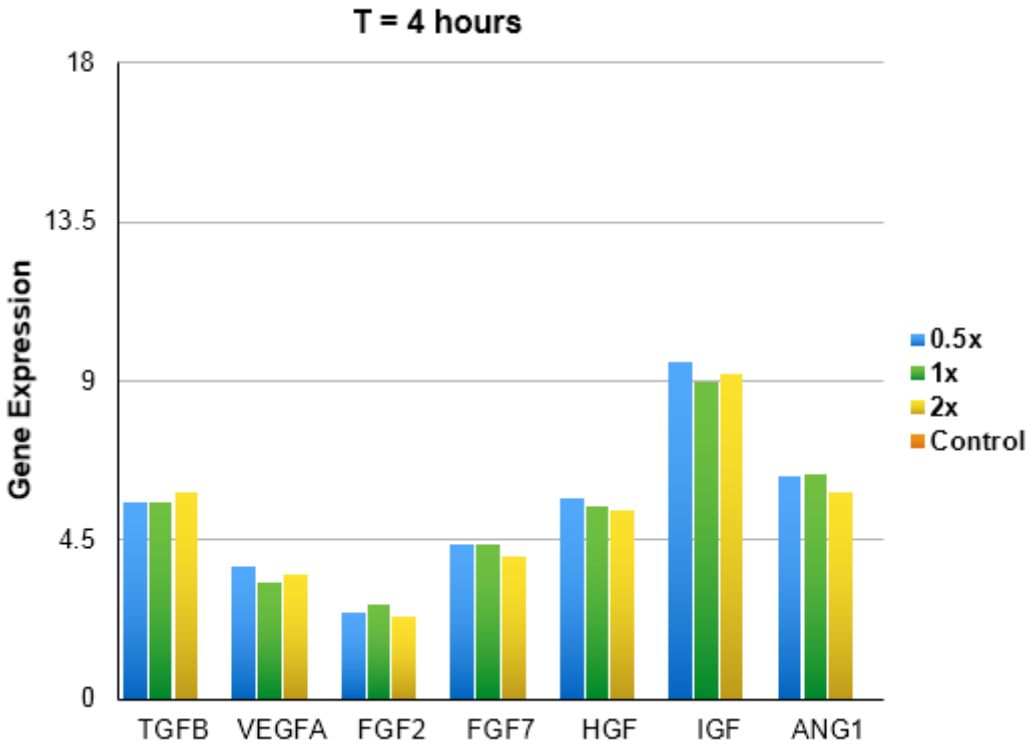

Figure 35. Gene expression at 4 hours for the control and experimental groups for H8 cell line.

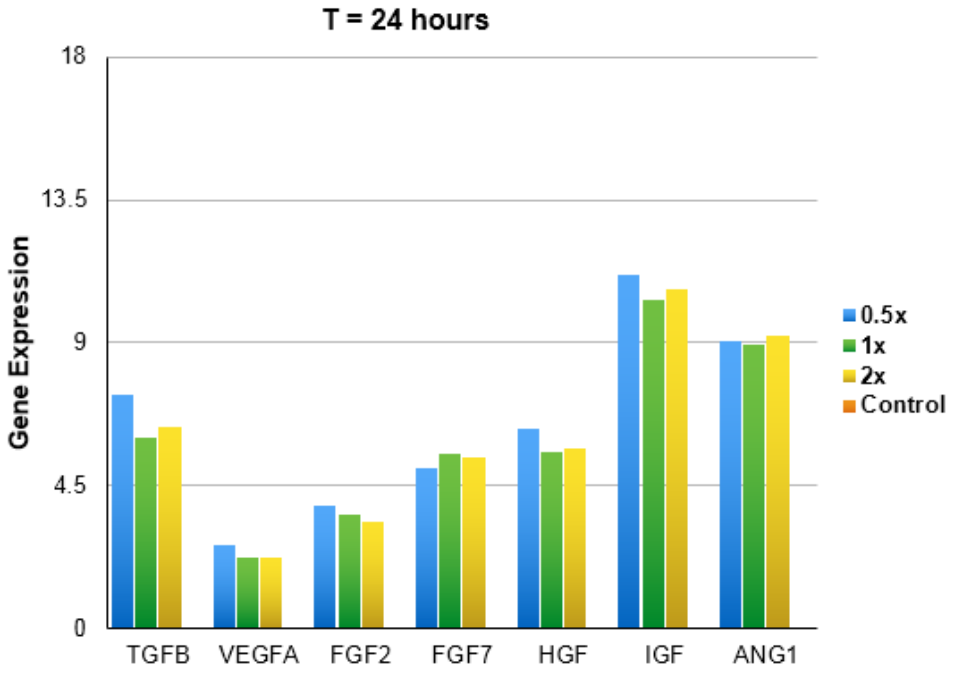

Figure 36. Gene expression at 24 hours for the control and experimental groups for H8 cell line.